EPRI (2004, 2006) Ground-Motion Model (GMM) Review Project

Responses to NRC Review Questions and Comments Dated July 3, 2013

July 30, 2013

CONTENTS

List of Response Authors 1

NRC Question 1 and Project Team Response 3

NRC Question 2 and Project Team Response 7

NRC Question 3 and Project Team Response 9

NRC Question 4 and Project Team Response 23

NRC Question 5 and Project Team Response 25

NRC Question 6 and Project Team Response 29

NRC Question 7 and Project Team Response 33

NRC Question 8 and Project Team Response 43

Appendix (submitted separately)

Errata for EPRI Technical Report *EPRI (2004, 2006) Ground-Motion Model (GMM) Review Project*, 3002000717, June 2013

AUTHORS

This document was prepared by the following investigators:

Principal Investigator Lead	Gabriel R. Toro
Project Manager	Lawrence A. Salomone
Principal Investigators	Martin Chapman Robin K. McGuire Gabriel R. Toro Robert R. Youngs
Database Manager	Serkan B. Bozkurt
Technical Support	J. Carl Stepp

Question 1: Section 7.10 contains a discussion of the development and rationale for the updated aleatory uncertainty (sigma) model used in the 2013 GMM update. The EPRI (2006) model for aleatory uncertainty was based on preliminary PEER NGA models for sigma from active tectonic regions with adjustments that account for differences between active and stable tectonic regions. The model for sigma used in the present study is again based on preliminary aleatory uncertainty models that have been under development for active tectonic regions as part of the NGA-West 2 project. Subsequent to the publication of the EPRI (2006) aleatory variability study, the final NGA-West sigma models were published and differed significantly from those referenced in the EPRI study. Specifically, magnitude dependence in sigma was incorporated into the models. Considering the preliminary state of the NGA-West 2 sigma models and the potential for future modifications, discuss the use of the NGA-West 2 sigma models as the basis for the aleatory uncertainty model used for the EPRI 2013 CEUS GMM.

Response:

One of the main conclusions of the EPRI (2006) study was that the empirical data set of strong motion recordings for active tectonic regions provides a better constraint on the aleatory variability of CEUS ground motions than the set of estimates based on parametric variability and limited CEUS data used to develop the EPRI (2004) aleatory variability model. EPRI (2006) used an average of the available values from the preliminary models developed during the PEER NGA Project to estimate the components of aleatory variability. As these values were based on statistical estimates from the analysis of observed data, they are subject to fluctuation as data sets are added to and modified and the associated models for median ground motions evolve. Figures 1-1 and 1-2 compare the average values of the estimates of the components of aleatory variability from the published versions of the four 2008 NGA GMPEs to the preliminary values used by EPRI (2006) for pseudo-spectral acceleration at 10 Hz and 1 Hz, respectively. As noted in the question, the final 2008 aleatory variability models incorporated magnitude dependence to some extent, while the preliminary models did not. This change accounts for some of the differences between the preliminary and final estimates, especially at large magnitudes.

The variation in estimates of aleatory variability as a function of data sets and analysis methods is well documented (e.g., Strasser et al., 2009). Therefore, it is not surprising that the major expansion of the size of the database in the NGA-West 2 Project, along with revisions in the associated median GMPEs, led to changes in the estimates of aleatory variability from those presented in the 2008 NGA models. As described in Section 7.10 of the report, the averages of the preliminary estimates of the components of aleatory variability from the NGA-West 2 Project were used to develop the update to the EPRI (2006) aleatory variability model. These values are also shown on Figures 1-1 and 1-2. Finally, completion of the NGA-West 2 database and finalized median models (as submitted to *Earthquake Spectra for an upcoming special issue*) resulted in changes in the estimates of the components of aleatory variability, as shown on Figures 1-1 and 1-2. The differences between the preliminary and final estimates of aleatory variability from the NGA-West 2 Project are generally less than the differences between the preliminary and final results from the 2008 NGA project, indicating that the preliminary results were in a more finalized state. Furthermore, the differences between the preliminary and final

estimates of aleatory variability from the NGA-West 2 Project are comparable to or smaller than the statistical uncertainty in estimating the variance parameters.

Along with the evolution of estimates of aleatory variability from empirical data, the approach to treatment of aleatory variability in PSHA is evolving. As described in Al Atik et al. (2010) and Rodriguez-Marek et al. (2013), the variability in recorded ground motions can be broken down into a number of contributing components, two of which are variability in response from site to site and variability in amplification at a given site. The accepted procedures for site-response analysis in Regulatory Guide 1.208 involve incorporating the uncertainty and variability in site response into the assessment of hazard at the foundation level of safety-related structures. As total aleatory variability estimated from empirical ground-motion data already includes a component related to site-response variability, there is a degree of double counting of uncertainties in using this aleatory variability to compute the reference hard-rock hazard.

Rodriguez-Marek et al. (2013) indicate that PSHA analysis is moving toward the use of what is termed “single station” sigma, in which the component of site-specific variability in site response is removed from aleatory variability used to compute the reference hard-rock hazard, and then is reintroduced in assessing the ground-motion hazard at the foundation level using site-specific information and its associated uncertainties. Rodriguez-Marek et al. (2013) demonstrate that values of single-station sigma and, in particular, the intra-event component, single station phi, are more stable across tectonic regions, across different tectonic environments, and among different investigators than are estimates of total aleatory variability. These results indicate that the single-station sigma concept may prove to be a more stable approach for developing aleatory variability models for PSHA.

Based on the above discussions, we conclude that the updated EPRI (2006) aleatory variability model presented in Section 7.10 of the report appropriately represents current estimates of the appropriate level of aleatory variability for computing the reference rock hazard at nuclear plant sites located in the CEUS. Although they are based on preliminary results from the NGA-West 2 Project, the values are generally within the statistical estimation uncertainty of the results from the finalized NGA-West 2 GMPEs. As demonstrated in Section 7.10 of the report, incorporation of multiple models to represent this level of statistical uncertainty is not needed for calculation of mean hazard. In addition, because the values are based on total observed aleatory variability, they are conservative when used in a ground-level hazard framework that incorporates additional uncertainty and variability in site response.

References

Al Atik, L., N. Abrahamson J.J. Bommer, F. Scherbaum, F. Cotton, and N. Kuehn, 2010. The variability of ground-motion prediction models and its components, *Seismological Research Letters* 81 (5), 794-801.

Electric Power Research Institute (EPRI), 2006. *Program on Technology Innovation: Truncation of the Lognormal Distribution and Value of the Standard Deviation for Ground Motion Models in the Central and Eastern United States*, EPRI Report 1013105, Technical Update, February, Palo Alto, Calif.

Rodriguez-Marek, A., F. Cotton, N. Abrahamson, S. Akkar, L. Al-Atik, B. Edwards, G. Montalva,

and H. Mousad, 2013 (in review). A model for single-station standard deviation using data from various tectonic regions, submitted to *Bulletin of the Seismological Society of America*.

Strasser, F.O., N.A. Abrahamson, and J.J. Bommer, 2009. Sigma: Issues, insights and challenges. *Seismological Research Letters* 80 (1), 40–54.

Figures Cited in the Responses

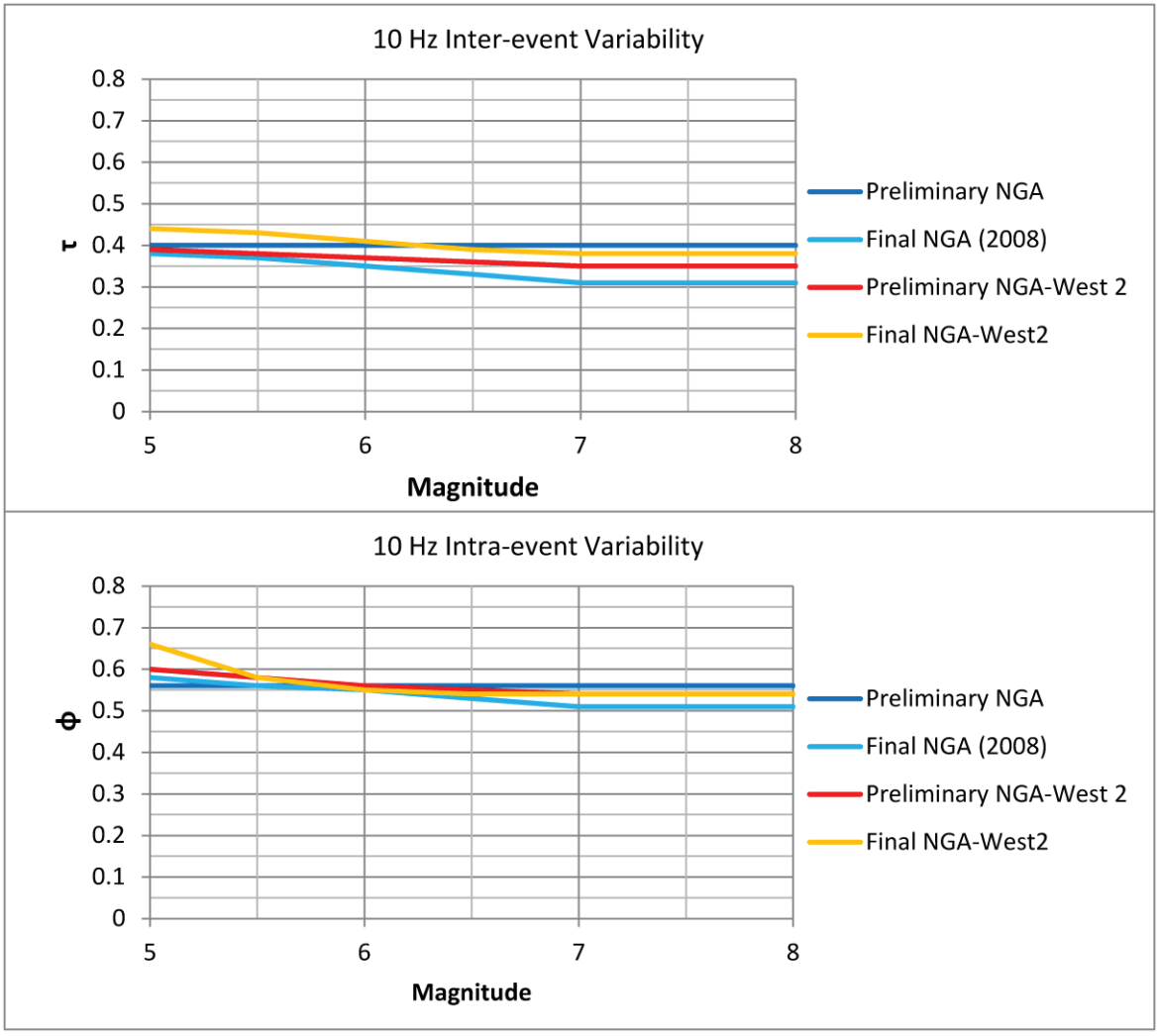

Figure 1-1: Comparison of evolving estimates of the components of aleatory variability for 10 Hz pseudo-spectral acceleration. Top plot shows standard error of inter-event variability, τ, in natural log units and bottom plot shows standard error of intra-event variability, φ, in natural log units.

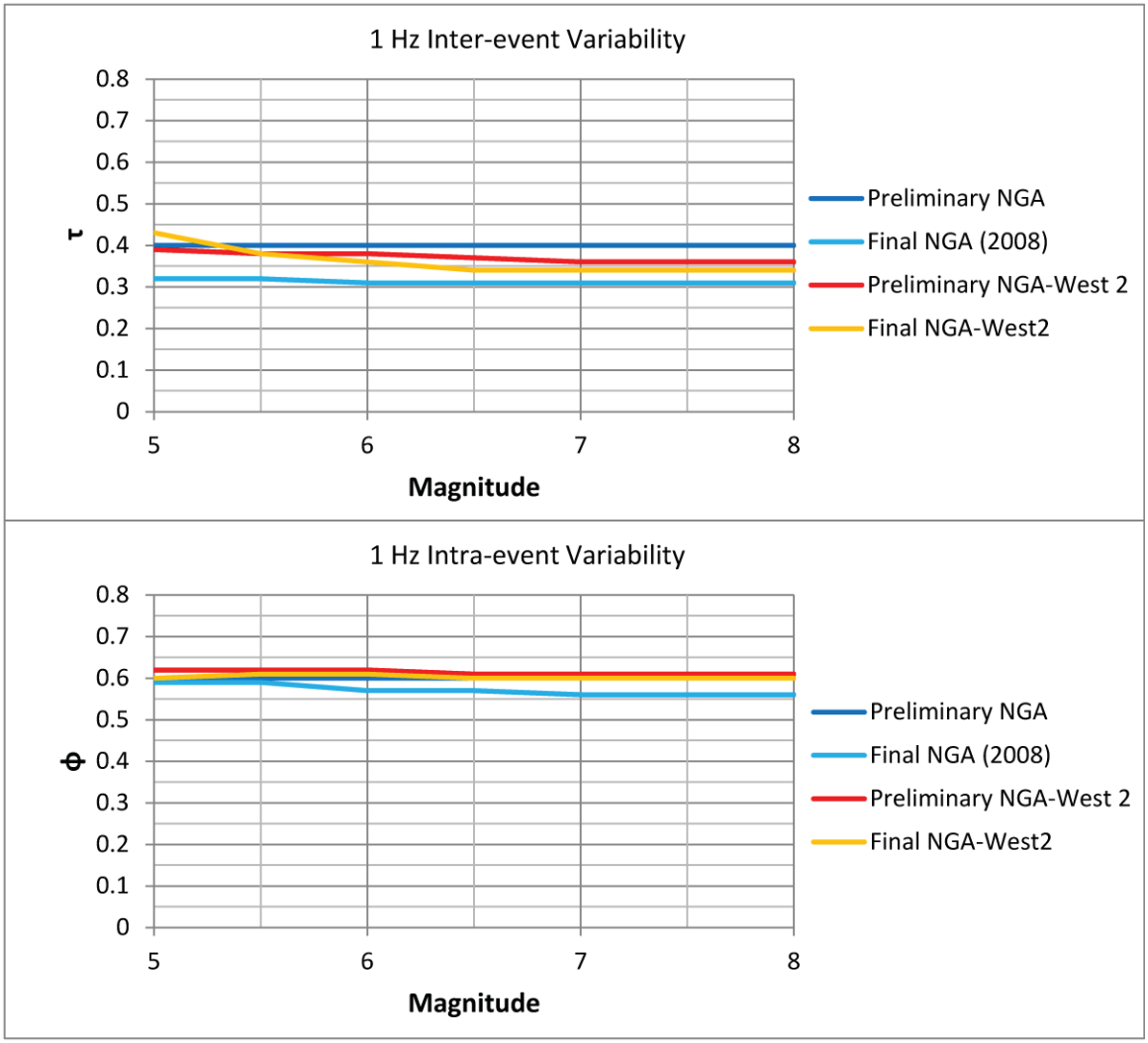

Figure 1-2: Comparison of evolving estimates of the components of aleatory variability for 1 Hz pseudo-spectral acceleration. Top plot shows standard error of inter-event variability, τ, in natural log units, and bottom plot shows standard error of intra-event variability, φ, in natural log units.

Question 2: The PEER NGA-East database includes estimates of epicentral and hypocentral distance measures for each earthquake recording. Section 7.2.4 of the EPRI (2013) GMM update provides a discussion of the procedures used estimate the rupture and Joyner-Boore distance measures that are applied to the NGA-East database given the epicentral and hypocentral distances. The two paragraphs following equation 7.2.4-2 describe the assumptions used to compute the vertical and horizontal location of the simulated ruptures and the simulation process. Please provide a clear definition of the hypocentral depth ratio and additional discussion on the simulation process.

Response:

The hypocentral depth ratio is the ratio of the vertical distance between the top of the rupture plane and the hypocenter to the vertical distance between the top and bottom of the rupture. The simulation process uses data about the rupture dimensions and orientation (if available) and realistic assumptions about these parameters (if event-specific data are not available) to calculate rupture and Joyner-Boore distances using the station and hypocentral locations. The intent of the simulation process is to produce estimates of the ground-motion measures used in the candidate GMPEs for those earthquakes that do not have estimates of the rupture plane. The simulated rupture geometries are used to compute distributions of rupture and Joyner-Boore distances. Median estimates are selected from the simulated distributions on the basis that the actual values are equally likely to be smaller or larger than the median value. The process was adopted by the NGA-West 2 Project for the development of distance parameters for small to moderate earthquakes for which only hypocentral distances were available (Ancheta et al., 2013). The process is well documented in Appendix B of Chiou and Youngs (2008). For most of the magnitudes and distances in the CENA data set considered in this study, the effect of these distance calculations is small.

References

Ancheta, T.D., R.B. Darragh, J.P. Stewart, E. Seyhan, W.J. Silva, B.S.-J. Chiou, K.E. Wooddell, R.W. Graves, A.R. Kottke, D.M. Boore, T. Kishida, and J.L. Donahue, 2013. PEER NGA-West 2 Database, Pacific Earthquake Engineering Research Center, PEER Report 2013/03, University of California, Berkeley.

Chiou, B.S.-J., and R.R. Youngs, 2008. *NGA Model for Average Horizontal Component of Peak Ground Motion and Response Spectra*, Pacific Engineering Research Center, College of Engineering, University of California, Berkeley, PEER Report 2008/09.

Question 3 (Parts a through e)

The EPRI (2004) GMPEs were developed to provide estimates of ground motion on hard-rock sites with shear-wave velocities of 2,800 m/s or greater, and this is also the reference site condition utilized in the EPRI (2013) GMM update. As there are no stations with measured or estimated shear-wave velocities at or near the 2,800 m/s in the PEER NGA-East database, a procedure has been used for the EPRI (2013) GMM update to adjust the recorded ground motions to the hard-rock reference condition. This adjustment was performed using two alternative approaches: an analytical approach for sites with a measured shear-wave velocity profile, and an empirical approach for sites where the shear-wave velocity is inferred from geologic conditions. In order for the staff to better understand these two approaches; please provide further clarification regarding the following:

Question 3a: *As described in Section 7.3 of the report, for sites located on stiff soil or soft/intermediate rock conditions site corrections were estimated. For sites with measured near-surface shear-wave velocity profiles an analytical approach was used to calculate site-specific amplification functions. For sites without measured near-surface shear-wave velocity profiles an empirical approach to estimate site correction factors for broad site classes was employed. The results obtained from these calculations were then used to correct the observed data prior to estimating the quality of the fit of each GMPE used in the updated GMM. There is significant uncertainty in estimating and extrapolating the shear-wave velocity profile to depth for the analytical approach and in classifying the sites in the empirical approach. The report recognizes these uncertainties and attempts to estimate them and propagate them through the process (as described in Section 7.4.3). However, the degree to which these uncertainties influence the final choice of weights in the model is not made clear. Please discuss and document the impact of the uncertainties on the final model.*

Response: In order to understand the effect of the uncertainties in site correction on the calculation of weights, it is useful to concentrate first on the diagonal terms of the covariance matrix, which are the most important terms, and consider the effect of the off-diagonal terms later. If the off-diagonal terms are neglected (resulting in a diagonal covariance matrix $\boldsymbol{\Sigma}_{\varepsilon}$ in Equation 7.4.3-5), the inverse of $\boldsymbol{\Sigma}_{\varepsilon}$ is also a diagonal matrix containing the reciprocals of the corresponding main-diagonal terms, so that Equation 7.4.3-5 may be written as

$$L(\boldsymbol{\varepsilon}_i) = \exp\left(-\frac{1}{2} \sum_j \sum_k \frac{{\varepsilon_{ijk}}^2}{\sigma^2 + {\sigma_{C,jk}}^2} \right) \qquad \text{(7.4.3-5a)}$$

where ε_{ijk} is the adjusted residual for GMPE *i*, earthquake *j,* and station *k*; $\sigma = \sqrt{\tau^2 + \phi^2}$ is the aleatory standard deviation for the rock motion (Section 7.10); and $\sigma_{C,jk}$ is the uncertainty in the adjustment factor for earthquake *j* at station *k*. In the analytical approach, $\sigma_{C,jk}$ has typical values of 0.4 to 0.7 (see Figures 7.3.1.2-4 through 7.3.1.2-6), which makes this term

comparable in size to $\sigma = \sqrt{\tau^2 + \phi^2}$. In the empirical approach, $\sigma_{C,jk}$ has typical values of 0.11 to 0.17 for soft-soil sites and 0 for intermediate- and hard-rock sites (see Table 7.5.2-1).

The presence of the term ${\sigma_{C,jk}}^2$ in the denominator of Equation 7.4.3-5a makes the equation less sensitive to the actual values of the squared residuals ${\varepsilon_{ijk}}^2$, so that the squared residuals are less diagnostic of a GMPE's fit to the data than they would be if the same residual values had been obtained directly on rock. This reduced sensitivity increases the tendency toward equal weights.

The following example illustrates the effect of the uncertainty in site response on the calculation of weights. Assume that there are two candidate GMPEs for which we wish to calculate weights based on 30 recordings obtained on soft- and intermediate-rock sites. Assume also that the root-mean-squared (rms) residuals (after adjusting to hard-rock site conditions using the analytical approach) are 0.8 and 0.9, respectively. Also, for the sake of simplicity, assume that $\sigma = 0.7$ and $\sigma_{C,jk} = 0.6$ (so that $\sigma^2 + {\sigma_{C,jk}}^2 = 0.85$) for all records (in practice, both quantities will differ somewhat from record to record as a result of the difference in magnitude, distance, site conditions, and frequency content of the recorded motion). The resulting values of the likelihood from Equation 7.4.3-5a are $\exp\left(-\frac{1}{2}30\frac{0.8^2}{0.85}\right) = 1.24\times10^{-5}$ and $\exp\left(-\frac{1}{2}30\frac{0.9^2}{0.85}\right) = 6.2\times10^{-7}$, resulting in weights of 0.95 and 0.05, respectively. If the same rms residuals had been observed without any site-response uncertainty, the denominator in Equation 7.4.3-5a would contain only the rock-site aleatory uncertainty, so that the values of the likelihood are $\exp\left(-\frac{1}{2}30\frac{0.8^2}{0.7^2}\right) = 3.1\times10^{-9}$ and $\exp\left(-\frac{1}{2}30\frac{0.9^2}{0.7^2}\right) = 1.7\times10^{-11}$, resulting in weights of 0.99 and 0.01, respectively.

In summary, the effect of the site-response uncertainty terms in the main diagonal of the covariance matrix is to make the squared residuals less diagnostic, thereby increasing the tendency toward equal weights.

The effect of the off-diagonal terms in the covariance matrix, which are always positive, is more difficult to visualize analytically, but is analogous to the effect of positive within-event correlation in the random-effect regression routinely used for developing empirical GMPEs (e.g., Brillinger and Preisler, 1984, 1985; Abrahamson and Youngs, 1992). The positive correlation between some residuals may be interpreted as reducing the effective sample size, which also has the effect of increasing the tendency toward equal weights for given values of the residuals.

Question 3b: *The GMM update report indicates in several places that sites with measured or inferred V_{S30} values less than 500 m/s are not used in the analysis. However, in the discussion of the analytical approach in Section 7.3.1.2 (pg. 7-13) the bulleted list of methods used to*

estimate kappa used in the EPRI SPID describes how soil sites with V_{S30} < 500 m/s are treated. Please clarify the treatment of these types of sites for the GMM update with regard to whether they are or are not used as part of the analysis.

Response: Profiles with measured V_{S30} < 500 m/s were not used in the analytical approach. The description of how kappa is calculated for these profiles should not have been included in Section 7.3.1.1, Step 3, page 7-13, because it creates confusion. Removal of the two bullets from Section 7.3.1.1, Step 3, page 7-13, is noted in the errata for the report (see Appendix).

Question 3c: *In Section 7.3.3 of the report example amplification factors developed using the empirical and analytical methods are compared. It is not clear from the description provided in Section 7.3.3 how the empirical results shown in Figures 7.3.3-1 through -4 were developed. Please clarify how the empirical results were obtained. Specifically, clarify which of the three empirical Models was used how the residuals are computed (relative to EPRI 2004 or the update GMM).*

Response: The empirical results were obtained using Method 3 presented in Section 7.3.2 (i.e., Equations 7.3.2-3 and 7.3.2-4) and applied in Section 7.5.2 (see Equation 7.5.2-1 and Table 7.5.2-1). The median values shown for the empirical method (i.e., the middle horizontal lines) are the median values of C_{SR} over all GMPEs in Table 7.5.2-1. The empirical + sigma range includes both the standard error in C_{SR} and the model-to-model differences in C_{SR} (see Table 7.5.2-1 for both).

Question 3d: *In the last paragraph of Section 7.3.3, reference is made to Figure 7.3.3-5 which is from the NGA summary report of Abrahamson et al. (2008). The text indicates that the figure illustrates consistency with the proposed EPRI (2013) amplification factors. Provide clarification on whether the cited figure is the appropriate figure and supports the conclusions in the text.*

Response: Figure 7.3.3-5 is the appropriate figure. Figure 7.3.3-5 shows a monotonic decrease in amplification factors with increasing V_{S30}, which is the same pattern shown by the analytical and empirical amplification factors in Figures 7.3.3-1 through 7.3.3-4 (i.e., amplification factors of 1.6 to 2 between V_{S30} values of 500 and 1,500 m/s). The empirical and NGA amplification factors saturate at 1,500 m/s, and we interpret this saturation as a consequence of not having sufficient recordings from hard-rock sites.

Question 3e: *In Section 7.4.3.1 the report describes the process used in the calculation of weights for a particular frequency, cluster, and approach for adjusting to reference site conditions. This approach works with the amplitude predicted for each GMPE (equation 7.4.3-1). In Equation 7.4.3-3 the process for including the uncertainty in site adjustment is described. The term $\delta_{C,jk}$ is identified as the uncertainty in the adjustment factor to reference rock for the k* th *station (with standard deviation $\sigma_{C,jk}$). However, these terms are non-zero only for the empirical soft-rock stations (see Figures 7.3.3-1 through -4). Also, following the description in Section 7.3, for a single station and a single GMPE using the empirical approach*

the uncertainty in the amplification is zero. The uncertainty for a single GMPE arises from looking at residuals across all stations of a given site type (soft-rock). Provide additional clarification on how this approach to incorporating the uncertainty is employed for the sites with empirical site corrections. In addition, provide additional clarification and discussion of how the standard deviation described in Section 7.4.3.1 is developed for the empirical stations.

Response: The approach for the incorporation of site-response uncertainty in the calculation of weights for the empirical approach is the same approach described in the response to Question 3a, with the following minor differences:

- The uncertainty $\sigma_{C,jk}$ is zero for intermediate- and hard-rock sites and is smaller than the analytically derived uncertainty for soft-rock sites.
- The uncertainty $\sigma_{C,jk}$ is slightly different for different GMPEs (see Table 7.5.2-1).

The uncertainty $\sigma_{C,jk}$ represents the standard error of estimation of C_{SR} in the linear, mixed-effects regression solution of Equation 7.3.2-3. This uncertainty depends on the scatter of the residuals and on the number of records in the soft-rock and intermediate- plus hard-rock categories.

References

Abrahamson, N., and W. Silva, 2008. Summary of the Abrahamson & Silva NGA ground-motion relations, *Earthquake Spectra* 24 (1), 67-97.

Abrahamson, N.A., and R.R. Youngs, 1992. A stable algorithm for regression analyses using the random effects model, *Bulletin of the Seismological Society of America* 82 (1), 505-510.

Brillinger, D.R., and H.K. Preisler, 1984. An exploratory analysis of the Joyner-Boore attenuation data, *Bulletin of the Seismological Society of America* 74 (4), 1441-1450.

Brillinger, D.R., and H.K. Preisler, 1985. Further analysis of the Joyner-Boore attenuation data, *Bulletin of the Seismological Society of America* 75 (2), 611-614.

Other Material Cited in the Responses

$$\ln(\text{Residual})_{\text{Model3}} = C_0 + C_{SR}F_{SR} + \varepsilon_{i,j} \tag{7.3.2-3}$$

$$\varepsilon_{ij}^{\text{empirically adjusted}} = \varepsilon_{ij} - C_{SR}F_{jk}^{SR} \tag{7.3.2-4}$$

$$\varepsilon_{ijk} = \ln[\text{Ampl}_{ijk}]_{\text{observed}} - \ln[\mu_{ijk}] \tag{7.4.3-1}$$

$$\varepsilon_{ijk} = \ln[\text{Ampl}_{ijk}]_{\text{adjustedobservation}} - \ln[\mu_{ijk}] = \delta B_j + \delta W_{jk} + \delta C_{jk} \tag{7.4.3-3}$$

$$L(\boldsymbol{\varepsilon}_i) = \exp\left(-\frac{1}{2}\boldsymbol{\varepsilon}_i{}^T \boldsymbol{\Sigma}_{\boldsymbol{\varepsilon}}{}^{-1}\boldsymbol{\varepsilon}_i\right) \tag{7.4.3-5}$$

$$\varepsilon_{ij}^{\text{empirically adjusted}} = \varepsilon_{ij} - C_{SR}F_{jk}^{SR} \tag{7.5.2-1}$$

Table 7.5.2-1
Soft-Rock Scaling Factors Used for Empirical Site Adjustments

GMPE	Soft-Rock Scaling Factor C_{SR} for Frequency of:					
	25 Hz	**10 Hz**	**5 Hz**	**2.5 Hz**	**1 Hz**	**0.5 Hz**
SSCCSC	0.43 ± 0.17	0.11 ± 0.14	0.09 ± 0.13	0.25 ± 0.13	0.34 ± 0.13	0.59 ± 0.12
SSCVS	0.44 ± 0.17	0.10 ± 0.14	0.09 ± 0.13	0.25 ± 0.13	0.34 ± 0.12	0.59 ± 0.12
TEL	0.44 ± 0.16	0.12 ± 0.13	0.12 ± 0.13	0.27 ± 0.12	0.34 ± 0.11	0.57 ± 0.11
FEL	0.46 ± 0.16	0.16 ± 0.13	0.15 ± 0.12	0.30 ± 0.12	0.36 ± 0.11	0.58 ± 0.11
A08′	0.35 ± 0.15	0.16 ± 0.13	0.15 ± 0.12	0.29 ± 0.11	0.34 ± 0.12	0.60 ± 0.11
SDCS	0.44 ± 0.17	0.11 ± 0.14	0.10 ± 0.13	0.25 ± 0.13	0.34 ± 0.13	0.59 ± 0.12
AB06′	0.50 ± 0.17	0.19 ± 0.14	0.16 ± 0.13	0.30 ± 0.12	0.35 ± 0.12	0.56 ± 0.11
PZT	0.49 ± 0.17	0.20 ± 0.15	0.17 ± 0.13	0.31 ± 0.12	0.36 ± 0.12	0.56 ± 0.11
SEL	0.43 ± 0.18	0.18 ± 0.14	0.16 ± 0.12	0.31 ± 0.12	0.38 ± 0.13	0.63 ± 0.13

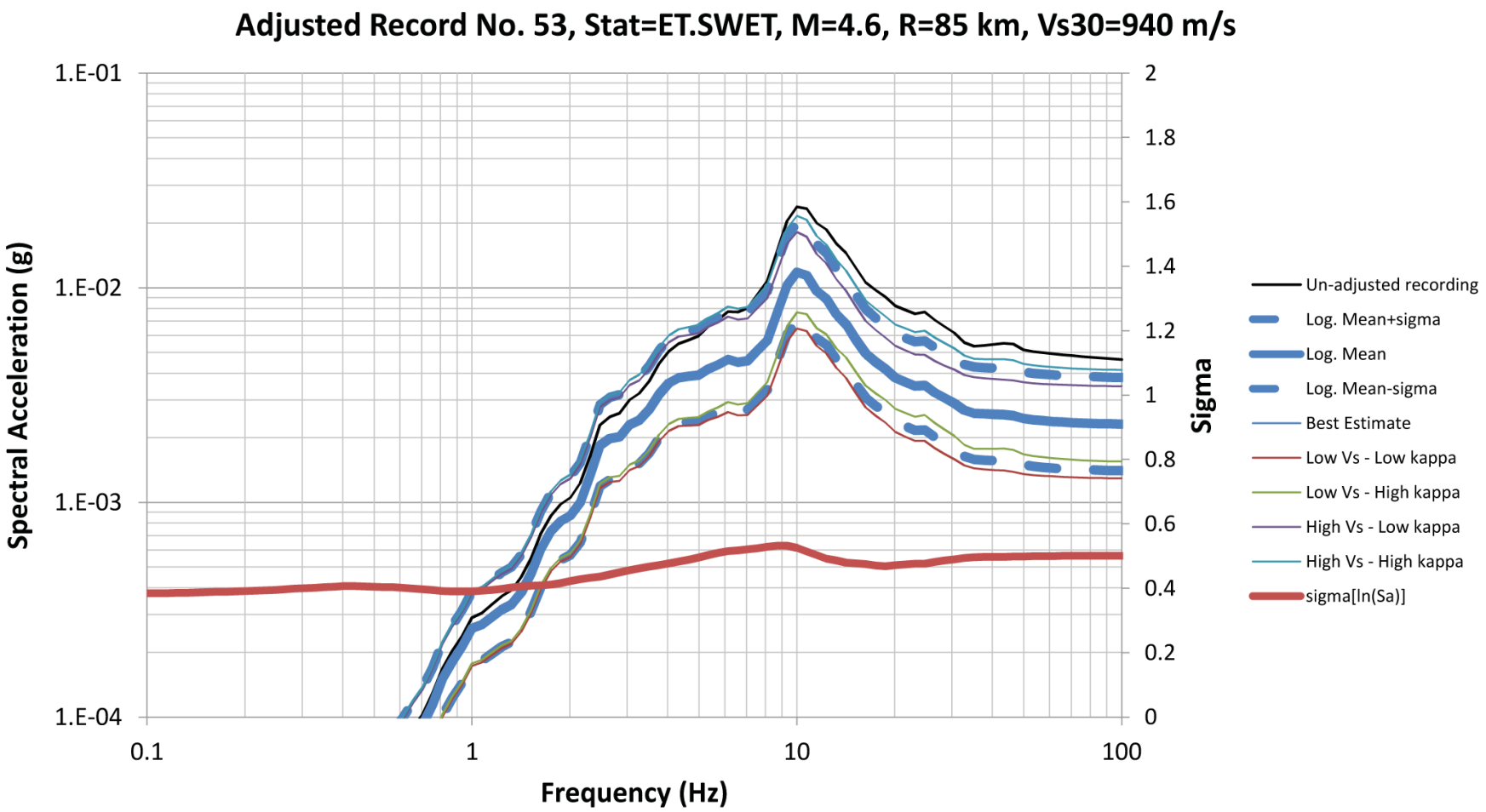

Figure 7.3.1.2-4
Adjusted and original response spectra for an M 4.6 earthquake recorder at rock station ET.SWET at a distance of 85 km

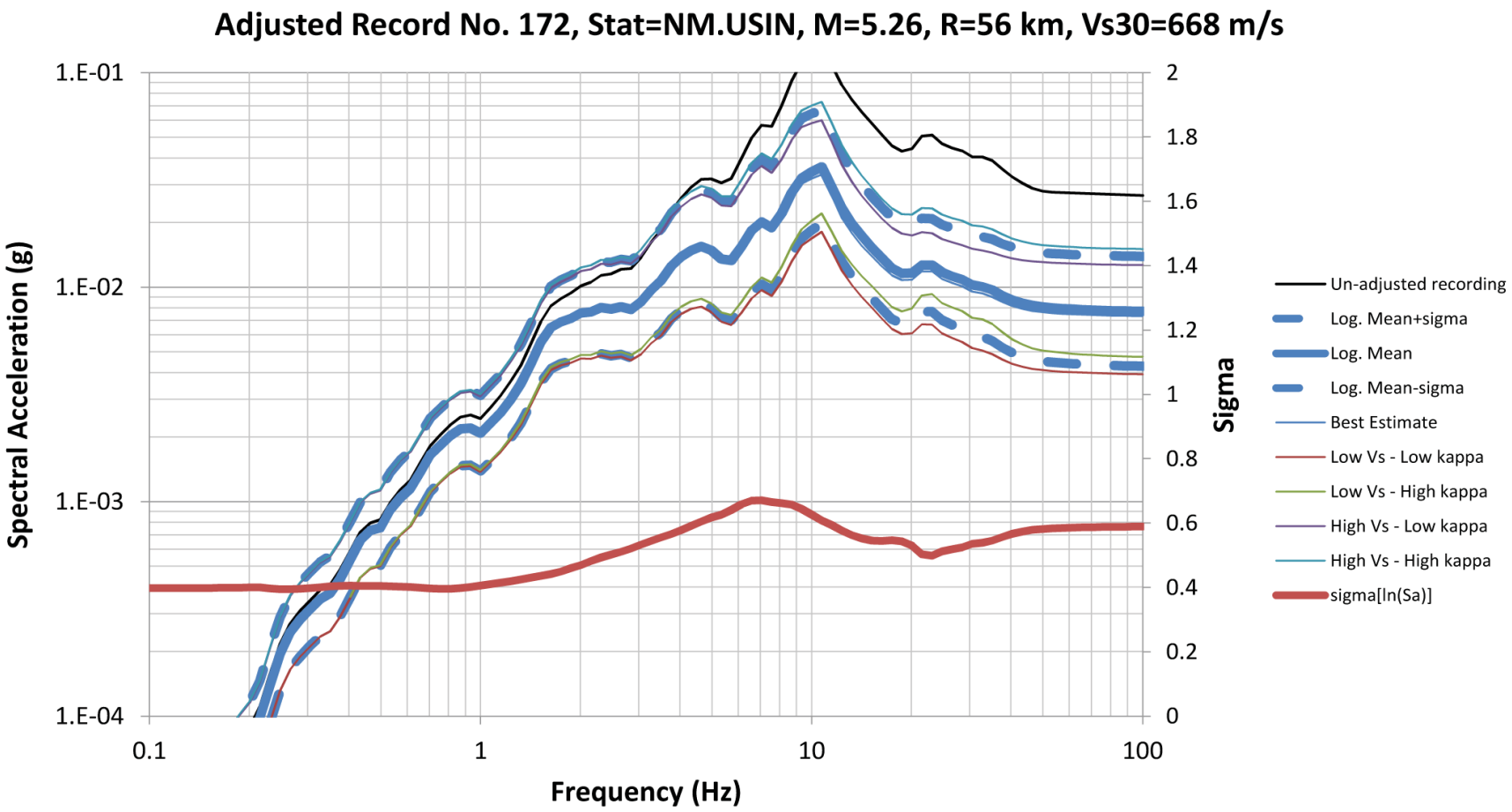

Figure 7.3.1.2-5
Adjusted and original response spectra for an M 5.3 earthquake recorder at rock station NM.USIN at a distance of 56 km

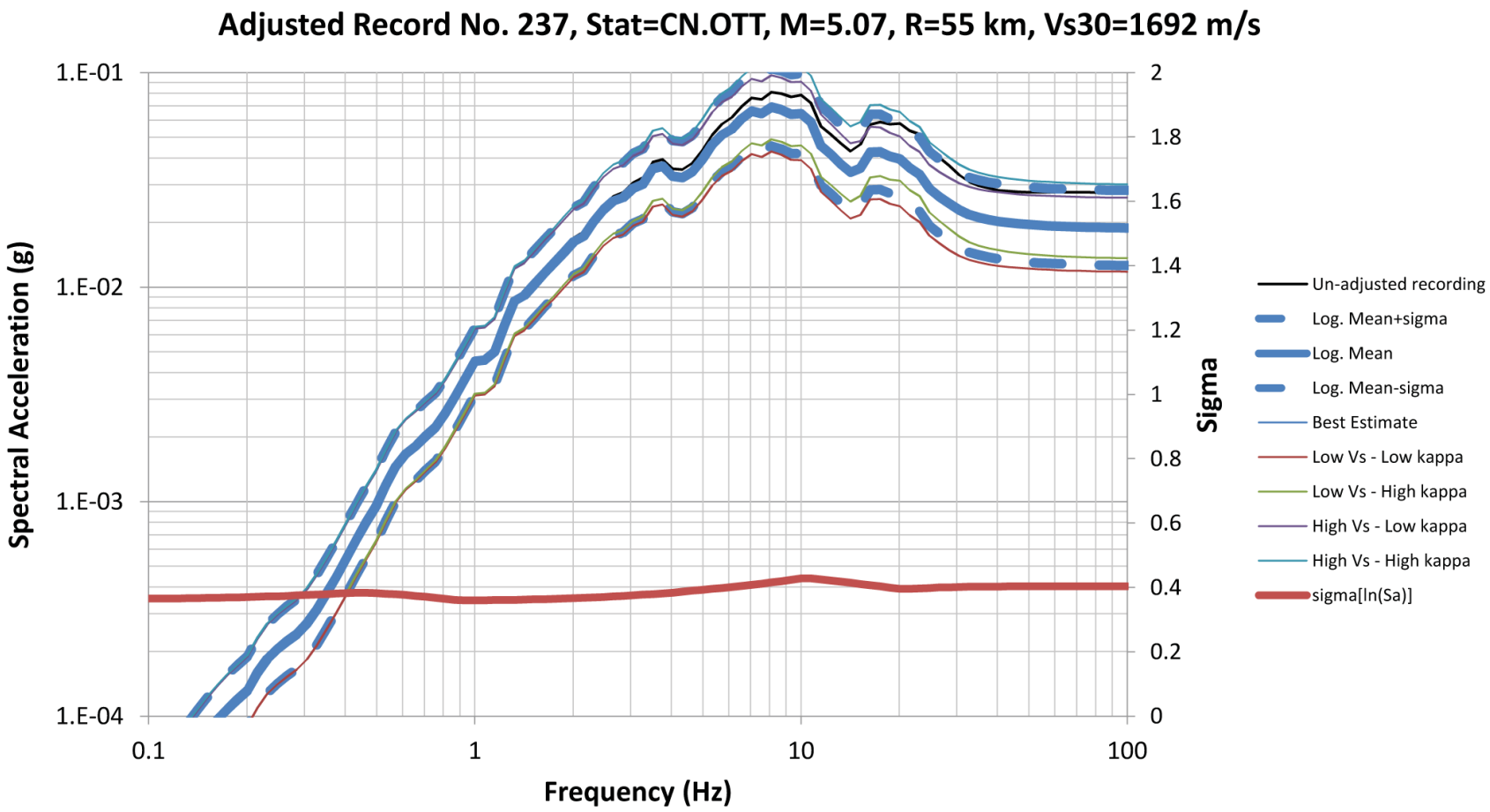

Figure 7.3.1.2-6
Adjusted and original response spectra for an M 5.1 earthquake recorder at rock station CN.OTT at a distance of 55 km

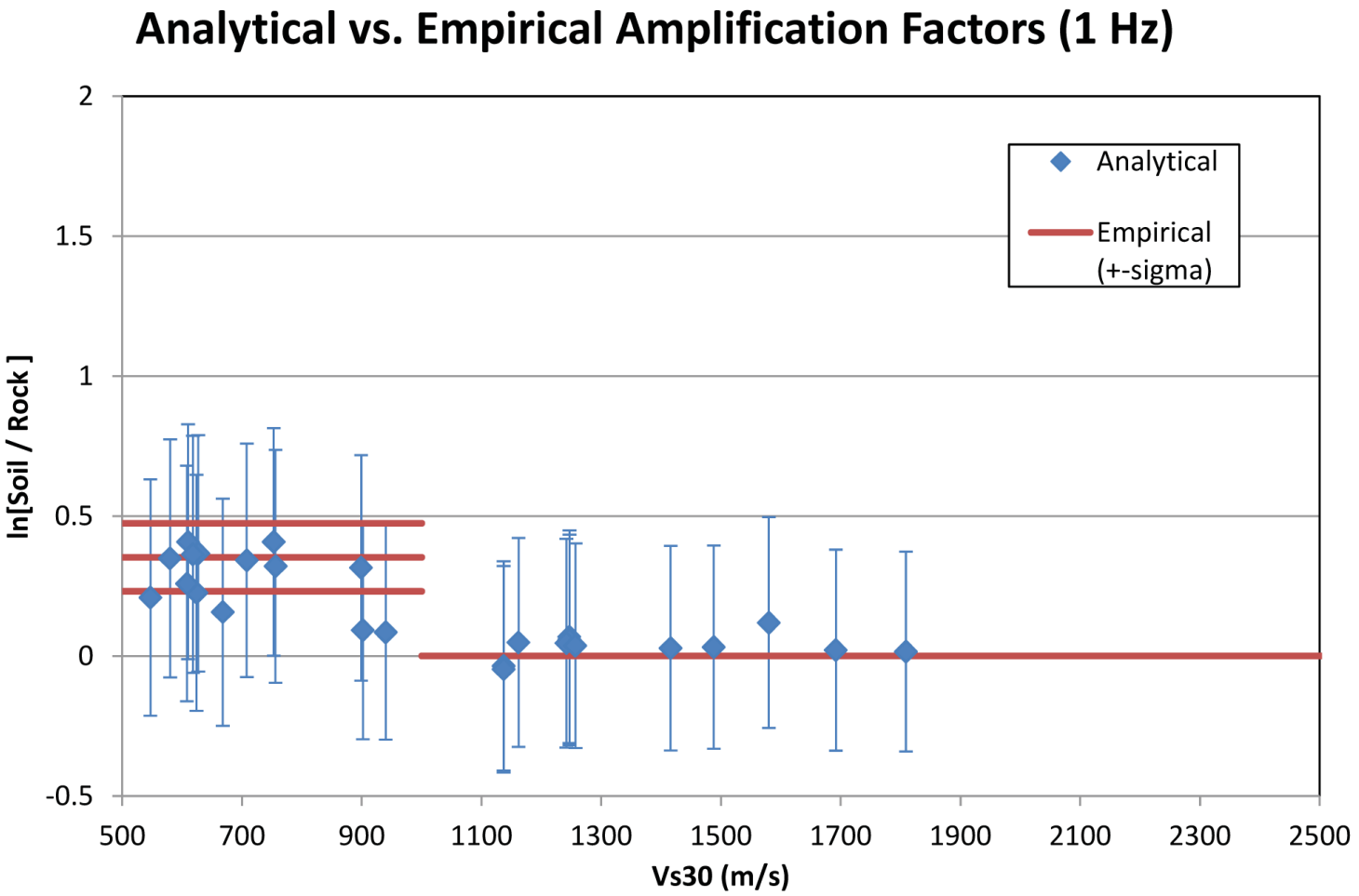

Figure 7.3.3-1
Comparison of analytical and empirical amplification factors for 1 Hz. Results shown are based on data for M ≥ 4.75 and R_{JB} ≤ 500 km

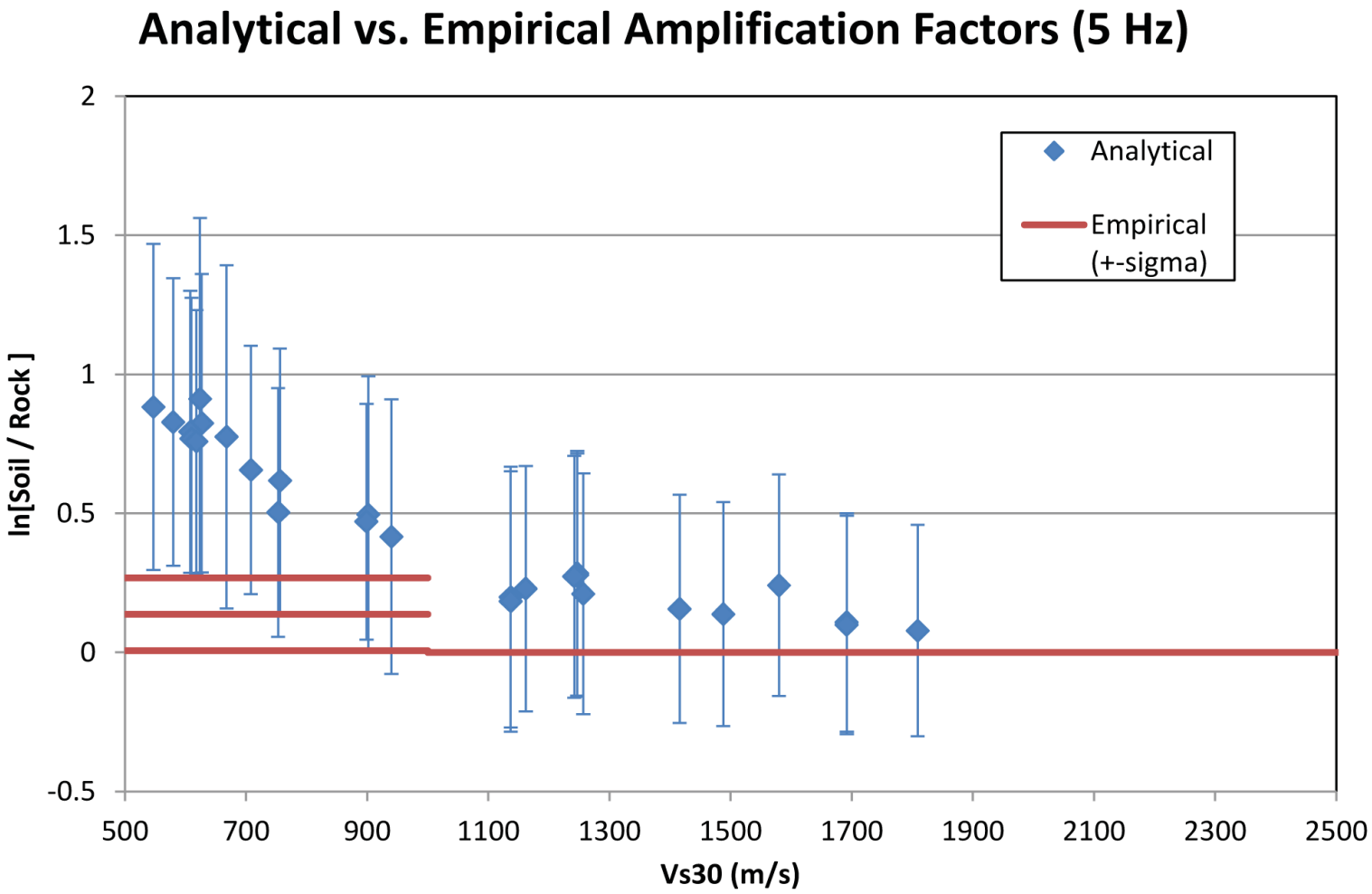

Figure 7.3.3-2
Comparison of analytical and empirical amplification factors for 5 Hz

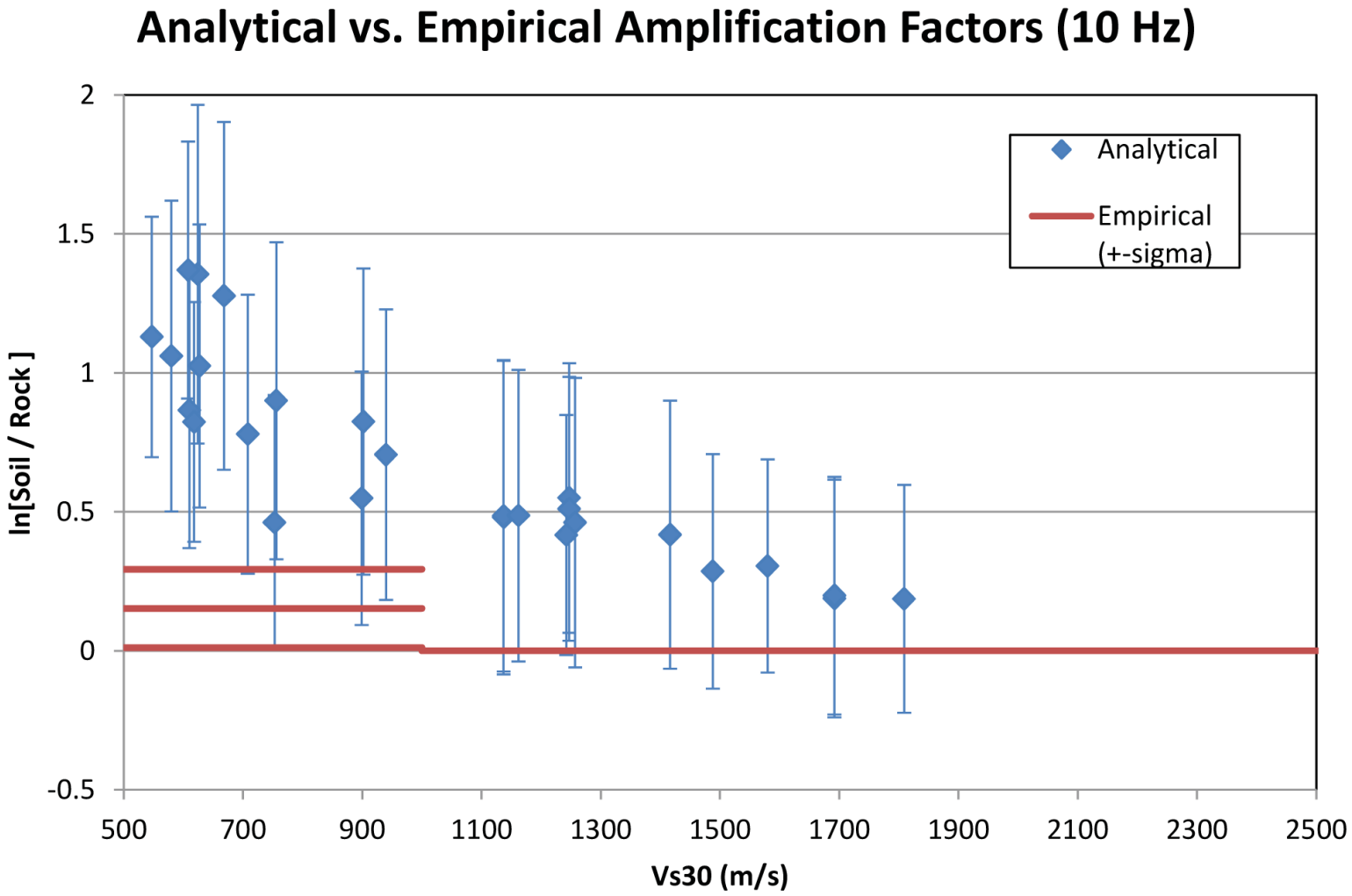

Figure 7.3.3-3
Comparison of analytical and empirical amplification factors for 10 Hz

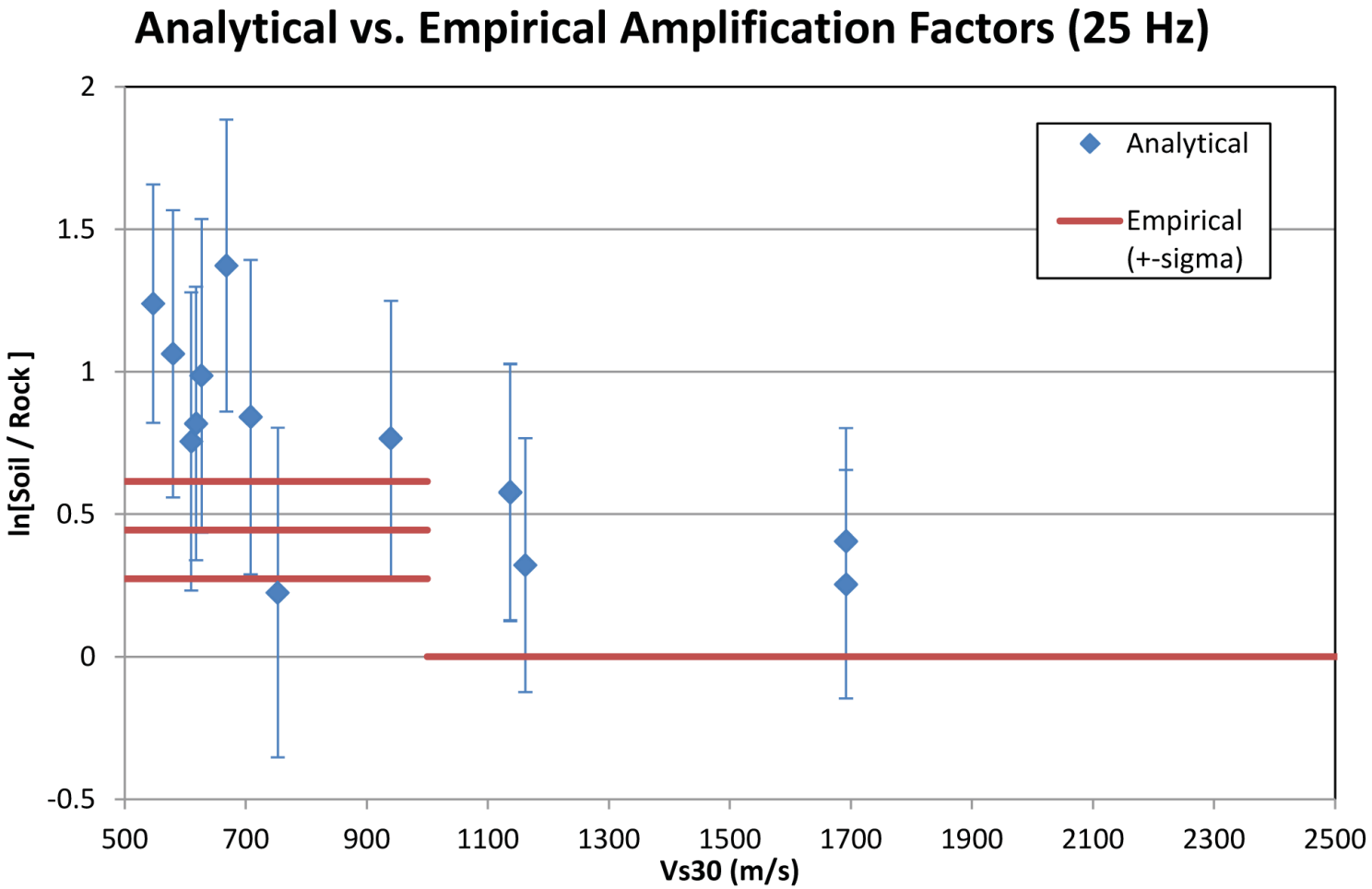

Figure 7.3.3-4
Comparison of analytical and empirical amplification factors for 25 Hz

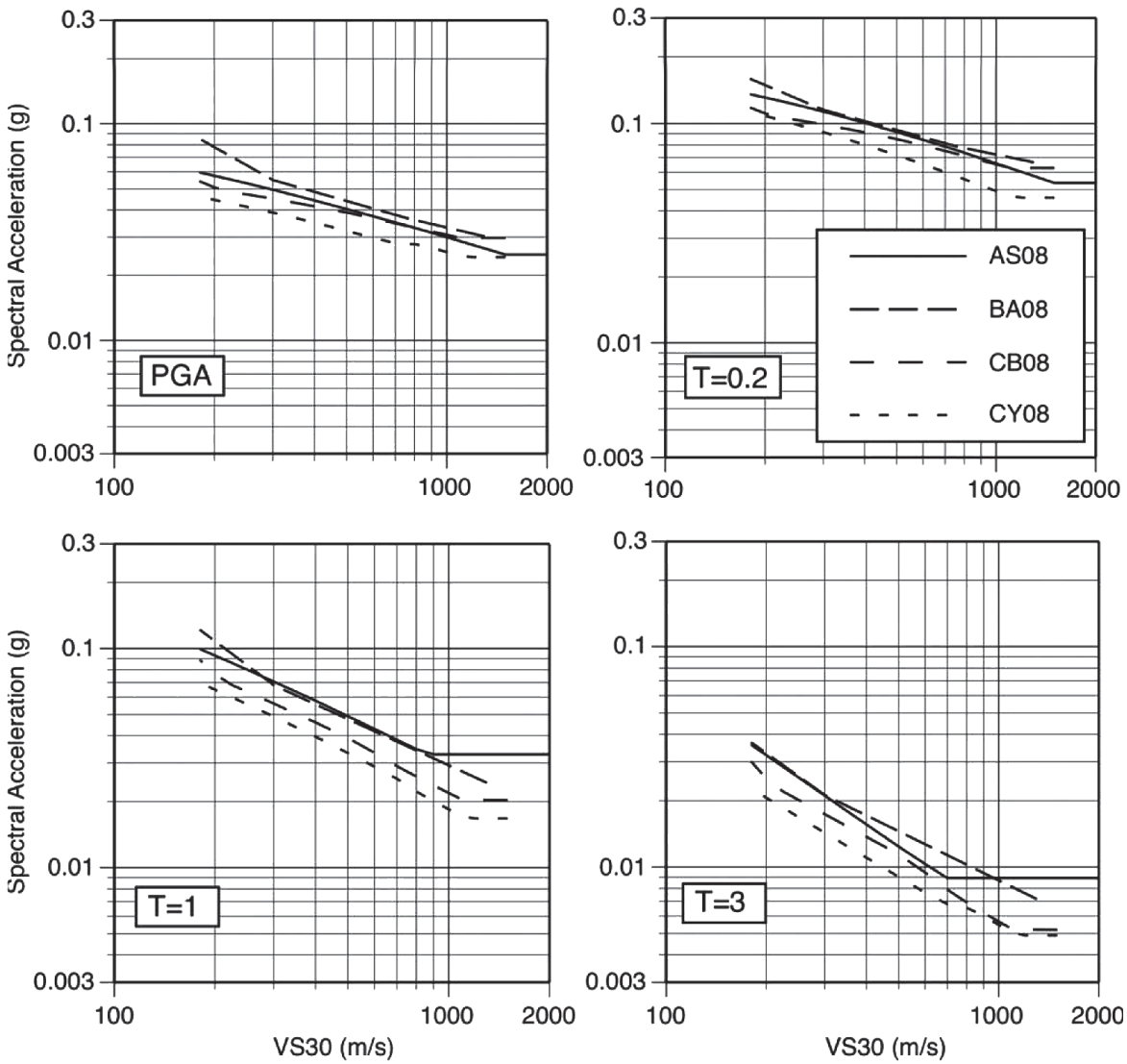

Figure 7.3.3-5
NGA amplification factors for magnitude 6 at 100 km. Modified from Abrahamson et al. (2008)

Question 4: In Section 7.6.2 the cluster median GMMs are developed and presented. Equation 7.6.2-2 specifies the functional form for Cluster 2. This equation, specifically the expression for R', does not match the equation in the Hazard Input Document (Appendix I of the report). Please provide an explanation for the discrepancy.

Response:
The equation in the HID is correct and Equation 7.6.2-2 in the text is incorrect. This error is noted in the errata for the report (see Appendix).

Question 5: In Section 7.11.1 the EPRI GMM update report describes the rationale for developing a separate GMPE for the Gulf Coast and the boundaries of that region. Specifically, the report notes: “The southern part of the Gulf Coastal Plain is underlain by thinned continental crust that was affected by early Mesozoic extensional tectonics associated with the formation of the Gulf of Mexico (Salvador, 1991a; EPRI/DOE/NRC, 2012). This crustal thinning can be expected to have some impact on the propagation of the Lg phase.” The report further states that: “An additional factor affecting attenuation in this region is the presence of an extremely thick Mesozoic and Cenozoic sedimentary section in the region affected by crustal extension. Near the coastline in Texas, Louisiana, and Mississippi, the sedimentary section reaches a thickness in excess of 10 km (Salvador, 1991b).”

While the above statements are supported by the references in a broad sense, it is not clear that the Florida peninsula falls into the same geophysical and geological category as the rest of the Gulf Coast. While very thick sequences of geologically young sediments do exist under the Gulf Coast of Texas, Louisiana, Mississippi, and Alabama, these same types of deposits are not present beneath much of Florida. Much of the basis for developing the correction factors to apply to the Mid-Continent GMPEs (the different regional Q values) comes from the analysis of data from the EarthScope Travelling Array. The TA is just now beginning to be deployed in the Florida region. Hence, data is not available to verify regional Q values in the Florida peninsula.

Given that: the southeastern boundary of the updated Gulf Coast region differs from that utilized in the EPRI (2004) model, basic data to very regional Q-values in Florida are not available, and the thickness of the young sediments beneath the Florida peninsula is much less than that beneath the rest of the Gulf Coast, the definition of the southeastern boundary of the Gulf Coast attenuation region may be subject to considerable uncertainty Please provide additional discussion and justification for the proposed boundary in Florida.

Response:

There are two possible mechanisms for the observed low amplitudes of Lg in the Gulf region, as follows:

1. Lg phase blockage due to thinning/disruption of the crustal waveguide. Kennett (1986) has shown that structural boundaries that involve thinning of the crustal waveguide are particularly disruptive of Lg.

2. Anelastic attenuation caused by thick, low-velocity, low-Q sediments.

The basis for the Gulf region defined in this study is not sediment thickness. The ground-motion models are used to predict rock motions, in the absence of sediments, and the Q model was developed to reflect average properties of the crustal waveguide in the Gulf region, in the absence of the low-velocity sedimentary section.

The Gulf region defined in this study delineates the region of the southern United States that has experienced crustal extension and thinning (EPRI/DOE/NRC, 2012, Chapter 7, Sections 7.3.9 and 7.3.10). This region closely corresponds to the northern and eastern margins of the Gulf of Mexico structural basin, which underwent extensional tectonics in the Mesozoic, as described by the authors contributing to the Geological Society of America *Decade of North*

American Geology Project volume entitled *The Gulf of Mexico Basin (*Salvador, 1991a), with the inclusion of the Mississippi Embayment, a zone of earlier late Proterozoic extension to the north. The degree of crustal extension (and thinning) increases from the periphery of the region toward the center of the Gulf of Mexico basin. Within this region, both mechanisms mentioned previously for Lg attenuation are in effect to various degrees, depending on the location, and it is not possible to determine which is dominant at a given location. There is clear observational evidence from EarthScope TA stations that attenuation correlates with sediment thickness. However, sediment thickness tends to be correlated with early Mesozoic crustal extension/thinning in the Gulf region. For example, the onshore areas of thin transitional crust in coastal Texas and Louisiana are underlain by the thickest sections (up to 12 km) of Mesozoic and younger sedimentary material (Sawyer et al., 1991; Salvador, 1991b).

At this point it is unknown whether Lg blockage or anelastic attenuation is the dominant factor leading to observed small Lg amplitudes in those areas. Furthermore, much of the northern part of the region in northeastern Texas, northern Louisiana, and southern Arkansas is on thick transitional continental crust of the type that presumably underlies most, if not all, of Florida (Sawyer et al., 1991; Ewing, 1991; EPRI/DOE/NRC, 2012), where the sediment thickness is generally less than 5 km, yet the region exhibits appreciable attenuation of Lg. It would appear that minor changes in the crustal waveguide have significant impact on Lg amplitude.

The entire state of Florida lies within the Gulf of Mexico structural basin (Salvador, 1991c; Ewing, 1991; Sawyer et al., 1991). The Florida and Yucatan peninsulas and their adjacent offshore shelf regions together form the eastern and southern margins of the basin. They are both immense carbonate platforms, beneath which the deep structure is poorly known (Ewing, 1991). The Florida panhandle is underlain by uplifts and basins that formed due to Mesozoic extensional tectonics. The Apalachicola embayment is the southwestward extension of the South Georgia basin, a major early Mesozoic extensional terrane in Georgia and South Carolina (Chowns and Williams, 1983; McBride et al., 1989; Chapman and Beale, 2010). The Apalachicola embayment contains Jurassic and Cretaceous sediments with a thickness in excess of 2 km, overlain by approximately 1.6 km of Tertiary strata (Ewing, 1991).

The northern part of the Florida peninsula is dominated by the Ocala uplift, where lower Cretaceous sediments lie on Paleozoic sedimentary rock. Near the Georgia border the Paleozoic rocks are within 1 km of the surface. This feature is broadly similar to the Sabine uplift on the Texas-Louisiana border, a region that exhibits strong attenuation of Lg waves. The southern one-third of the Florida peninsula overlies the South Florida basin. Depth to basement is in excess of 6 km onshore in southern Florida, with more than 8 km of sediment accumulation on the offshore Florida platform that is underlain by highly extended continental crust (Ewing, 1991).

In summary:

Florida is the eastern margin of the Gulf of Mexico basin, a feature that was created by Mesozoic extensional tectonics. Florida is separated from cratonic North America, and the Paleozoic Appalachian orogenic belt, by two major structural boundaries:

1. The South Georgia basin (rift), a Mesozoic extensional terrane that appears to be linked to the opening of the Gulf of Mexico basin.

2. The Suwannee-Wiggins suture, which marks the late Paleozoic collision zone of Laurentia (which comprised cratonic North America and terranes that were accreted to the craton earlier in the Paleozoic) and Gondwana.

The geologic structure of Florida is intimately related to the rifting of Pangea and the development of the Gulf of Mexico basin. Wave propagation in the Gulf of Mexico structural basin to the west of the Florida peninsula is clearly distinct from that in the North American cratonic platform and Appalachian orogenic belt. The available data and evaluations thus support the conclusion that the Florida peninsula is part of the Gulf of Mexico structural basin in terms of both tectonic structure and Lg wave propagation. It is our position that the Florida peninsula should be included in the Gulf region of the EPRI (2004, 2006, 2013) Ground-Motion Model.

References

Chapman, M.C., and J.N. Beale, 2010. On the geologic structure at the epicenter of the 1886 Charleston, South Carolina earthquake, *Bulletin of the Seismological Society of America* 100, 1010-1030.

Chowns, T.M., and C.T. Williams, 1983. Pre-Cretaceous rocks beneath the Georgia Coastal Plain: Regional implications, in *Studies Related to the Charleston, South Carolina, Earthquake of 1886 – Tectonics and Seismicity*, U.S. Geological Survey Professional Paper 1313, L1-L42.

Electric Power Research Institute, U.S. Department of Energy, and U.S. Nuclear Regulatory Commission (EPRI/DOE/NRC), 2012. *Technical Report: Central and Eastern United States Seismic Source Characterization for Nuclear Facilities*, NUREG-2115.

Ewing, T.E., 1991. Structural framework, *in The Gulf of Mexico Basin*, edited by Amos Salvador, Volume J, Chapter 3, The Geology of North America, Geological Society of America, Boulder, Colorado, pp. 31-52.

Kennett, B.L.N., 1986. Lg waves and structural boundaries, *Bulletin of the Seismological Society of America* 76, 1133-1141.

McBride, J.H., K.D. Nelson, and L.D. Brown, 1989. Evidence and implications of an extensive early Mesozoic rift basin and basalt/diabase sequence beneath the southeast Coastal Plain, *Geological Society of America Bulletin* 101, 512-520.

Salvador, A. (editor), 1991a. *The Gulf of Mexico Basin,* The Geology of North America, Volume J, Geological Society of America, Boulder, Colorado, 568 pp.

Salvador, A., 1991b. Structure at the base and subcrop below Mesozoic Marine section, Gulf of Mexico basin, in *The Gulf of Mexico Basin*, edited by A. Salvador, Volume J, Plate 3, The Geology of North America, Geological Society of America, Boulder, Colo.

Salvador, A., 1991c. Introduction, in *The Gulf of Mexico Basin*, edited by A. Salvador, Volume J, Chapter 1, The Geology of North America, Geological Society of America, Boulder, Colo., pp. 1-12.

Sawyer, D.S., R.T. Buffler, and R.H. Pilger, 1991. The crust under the Gulf of Mexico basin, in *The Gulf of Mexico Basin*, edited by A. Salvador, Volume J, Chapter 4, The Geology of North America, Geological Society of America, Boulder, Colo. pp. 53-72.

Question 6 (Parts *a* through *g*)

Section 7.2.2.1 of the update EPRI GMM report briefly described the processing of the database, which was performed by Cramer as part of the NGA-East project, and references Cramer et al. (2013). In order for the staff to better understand the processing of the database, please respond to the following questions.

Question 6a: *Section 7.2.2.1 states that each recording was assigned a quality code, typically either "A" or "?", and that generally only records with quality level "A" were retained for this project. In addition, some recordings assessed as "?" were also retained for the project. Provide a description of the criteria used to (1) assess the quality of the recording and (2) retain recordings evaluated as questionable with a "?"*

Response: The definitions of quality levels are "A" – best quality with no known problems, and "?" – acceptable quality but possible problems with data, as indicated in the quality comment in the flat file at the end of entry line.

In order to maximize the number of recordings at the sites with V_S measurements, a few "?" designated records were retained after reviewing the quality comments and visual examination of the processed time histories to ascertain that the time histories looked realistic; no formal criteria were employed for this purpose.

Question 6b: *With respect to the NGA-East report (Cramer et al. (2013), clarify how pre-event noise was obtained for triggered instruments or other instruments with limited pre-event memory.*

Response: If little or no pre-event noise was in the record, no pre-event noise record could be generated. Filtering was based on signal spectral shape and experience with records having pre-event noise.

Question 6c: *The NGA-East strong motion processing report on page 9 states that a 2% cosine taper was used. Provide more detail on the use of the 2% cosine taper, especially for recordings with little or no pre-event memory.*

Response: The 2% cosine taper was applied to all records as a part of the standardized processing procedure. Records with peak ground motions at the beginning of the record (rare) were adjudged as quality "?" or rejected.

Question 6d: *Provide more detail on the signal processing filtering of the data (Butterworth?), including the order of the filter and the criteria for selecting the corner frequencies. In addition, provide more detail on the processing and combination of the two horizontal channels.*

Response: Signal processing was accomplished using the SAC software. Filtering was done as part of the instrument correction command TRANSFER using that command's frequency domain cosine filter with specified frequency corners and zero point frequencies a factor of two below or above the corner frequencies (low cut and high cut, respectively). Please refer to SAC

documentation of the TRANSFER command. As documented in the March 2008 NGA East reports on database development, this filtering was compared with the results of a four-pole Butterworth filter independently by Chris Cramer and Dave Boore, and the resulting time histories were found to be the same. The two horizontal channels were combined by calculating geometric averages.

Question 6e: *Provide further detail on the type of weak-motion recordings (broadband, short-period) retained for the project as well as the percentage relative to the strong-motion recordings.*

Response: A vast majority of the recordings in the database are broadband recordings with some selected short-period (1 s) recordings deemed usable due to high dynamic range in the digital recordings. Broadband recordings are mostly designated as BH* and HH* in the IRIS three-character component designator after the station ID. Short-period recordings are mostly designated as EH* or SH*, and accelerometers as HN* or HL* in this same component designator. See http://www.iris.edu/manuals/SEED_appA.htm for the definition of the designators used above. Note: * is used above to indicate any orientation.

Question 6f: *Elaborate on the filtering of long-periods and the potential for over prediction at large periods.*

Response: Filtering was chosen to remove obvious long-period noise from the pre-event portion of the time history and on the basis of signal-to-noise ratio. Filtered time histories were quality-control reviewed for noise problems after filtering, and the filter corners were adjusted to eliminate noise problems, if needed, and re-reviewed. Also, the longest period considered by the EPRI (2004, 2006) Ground-Motion Model (GMM) Review Project is 2 sec, so issues at longer periods are not a concern for this project.

Question 6g: *Provide further detail on the criteria for determining the size of the structure for the recording sites. Were the ANSS definitions used?*

Response:
Generally, the NGA-East Project did not perform a review of the size of the structure at the recording sites. Most of the data are from free-field recording sites. Some structural recordings are present in the database, particularly from the Mineral, VA, event from the Quake-Catcher (QC) and USGS National Strong Motion Program (NP) network designations. Because of the lower quality, most of the Quake-Catcher recordings are labeled of questionable quality. A comparison was made with nearby high-quality recordings, and the Quake-Catcher values were comparable with the high-quality recording values. Information on structure size, if available, is contained in the NGA-East file “NGAEastStationCompTable201208-27.xls” in the “Geological Information” field.

This project used the NGA-East information on structure size described above; stations with no information were considered free-field. The structure size code used follows that used in the

NGA and NGA-West 2 databases (e.g., Ancheta et al., 2013). The ANSS definitions were not used.

Reference

Ancheta, T.D., R.B. Darragh, J.P. Stewart, E. Seyhan, W.J. Silva, B.S.-J. Chiou, K.E. Wooddell, R.W. Graves, A.R. Kottke, D.M. Boore, T. Kishida, and J.L. Donahue, 2013. PEER NGA-West 2 Database, Pacific Earthquake Engineering Research Center, PEER Report 2013/03, University of California, Berkeley.

Question 7: Section 7.13 of the report provides sensitivity calculations to investigate the effects of a number of alternative assumptions. One alternative assumption that is not discussed is the overall impact of including additional uncertainty to account for magnitude scaling. Please provide a discussion of the relative importance of adding this factor, specifically with respect to the within-cluster epistemic uncertainty.

Response:

There are three contributors to within-cluster epistemic uncertainty:

1. Within-cluster model-to-model variability.
2. Data constraint uncertainty (magnitude-independent, but representative of magnitudes near **M** 5 only).
3. Magnitude-scaling uncertainty.

The within-cluster epistemic variance is calculated as the maximum of the variance from (1) and the sum of the variances from (2) and (3). The latter sum is labeled the cluster-independent epistemic uncertainty.

Examination of Figures 7.7.1-1 through 7.7.1-3 indicates that the within-cluster epistemic uncertainty based on model-to-model variability does not increase monotonically with magnitude for all clusters and frequencies, and a number of panels show low values (lower than 0.2 in a number of cases) for **M** 7 and 8 at distances from 1 km to 30 km.

Figure 7.7.1-9 shows the cluster-independent epistemic standard deviation calculated as the sum of the data constraint uncertainty and the magnitude scaling uncertainty. The increase in epistemic uncertainty with increasing magnitude shown on this figure is due entirely to the inclusion of the magnitude-scaling uncertainty.

Comparing the within-cluster epistemic uncertainty on Figures 7.7.1-10 through 7.7.1-13 to Figure 7.7.1-9, one observes that for Clusters 1, 3, and 4, and for distances from 1 km to at least 100 km, the combined within-cluster epistemic uncertainty is being controlled by the cluster-independent epistemic standard deviation.

Examining the values on the figures discussed above, one can conclude that the effect of removing the magnitude-scaling uncertainty would have the following effects for Clusters 1, 3, and 4:

- A nearly magnitude-independent within-cluster epistemic uncertainty at distances from 10 km to 30 km.
- A reduction in the within-cluster epistemic uncertainty for **M** 7 and 8 at distances from 1 km to 30 km. For **M** 8, the size of this reduction is approximately 0.12 natural log units, which translates into a factor of approximately exp(–0.12*1.645) or 0.82 on the high (or 95%) GMPE for each cluster, and a reciprocal factor of 1.22 on the low (or 5%) GMPE. Because this reduction affects only the 95% and 5% GMPEs, and because most of the hazard for exceedance frequencies of GMRS interest comes from lower magnitudes (particularly for high frequencies), the effect of this reduction is small.

In summary, the magnitude scaling uncertainty is a major contributor to the epistemic uncertainty at larger magnitudes in the updated ground-motion model.

Figures Cited in the Response

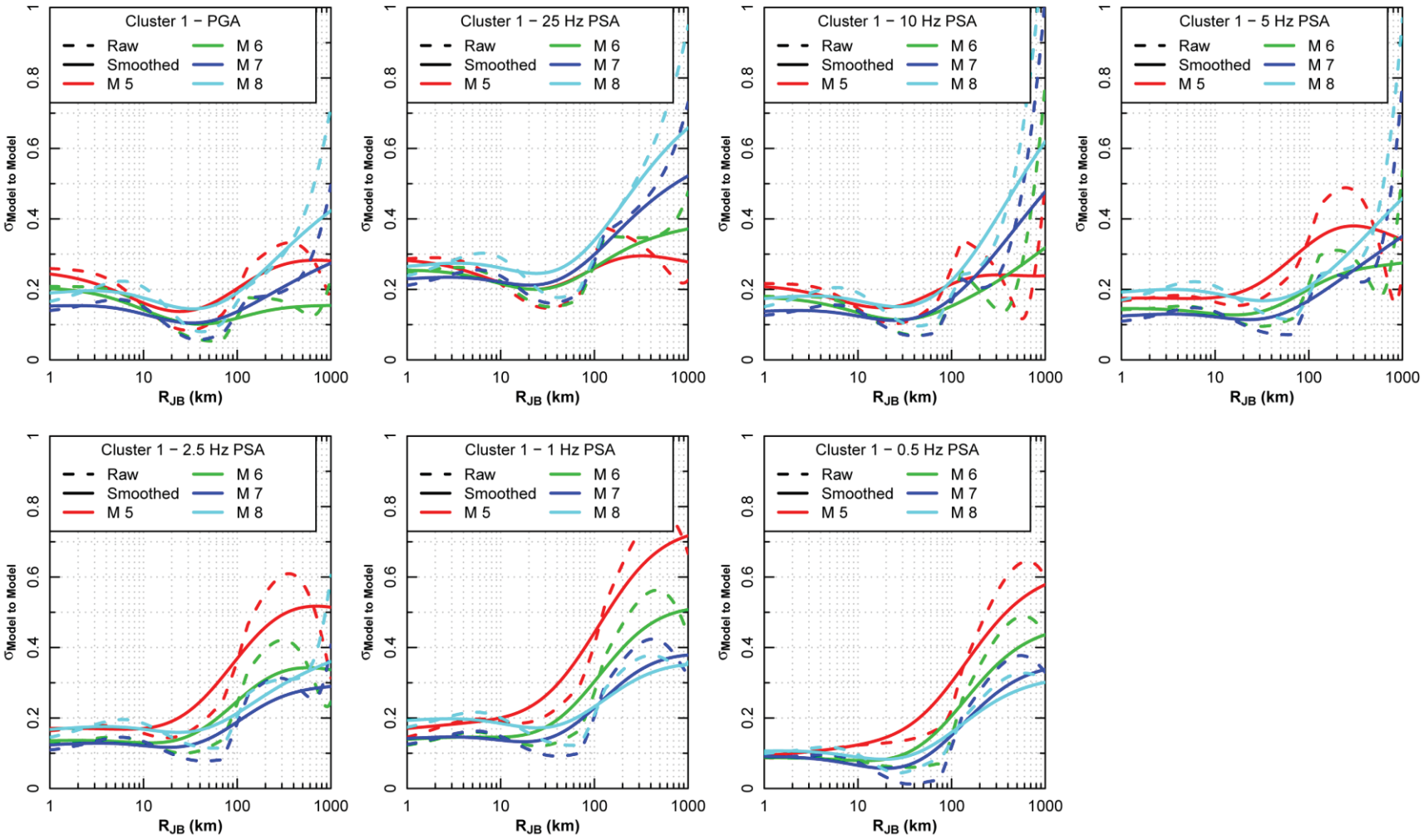

Figure 7.7.1-1
Model-to-model variability for Cluster 1

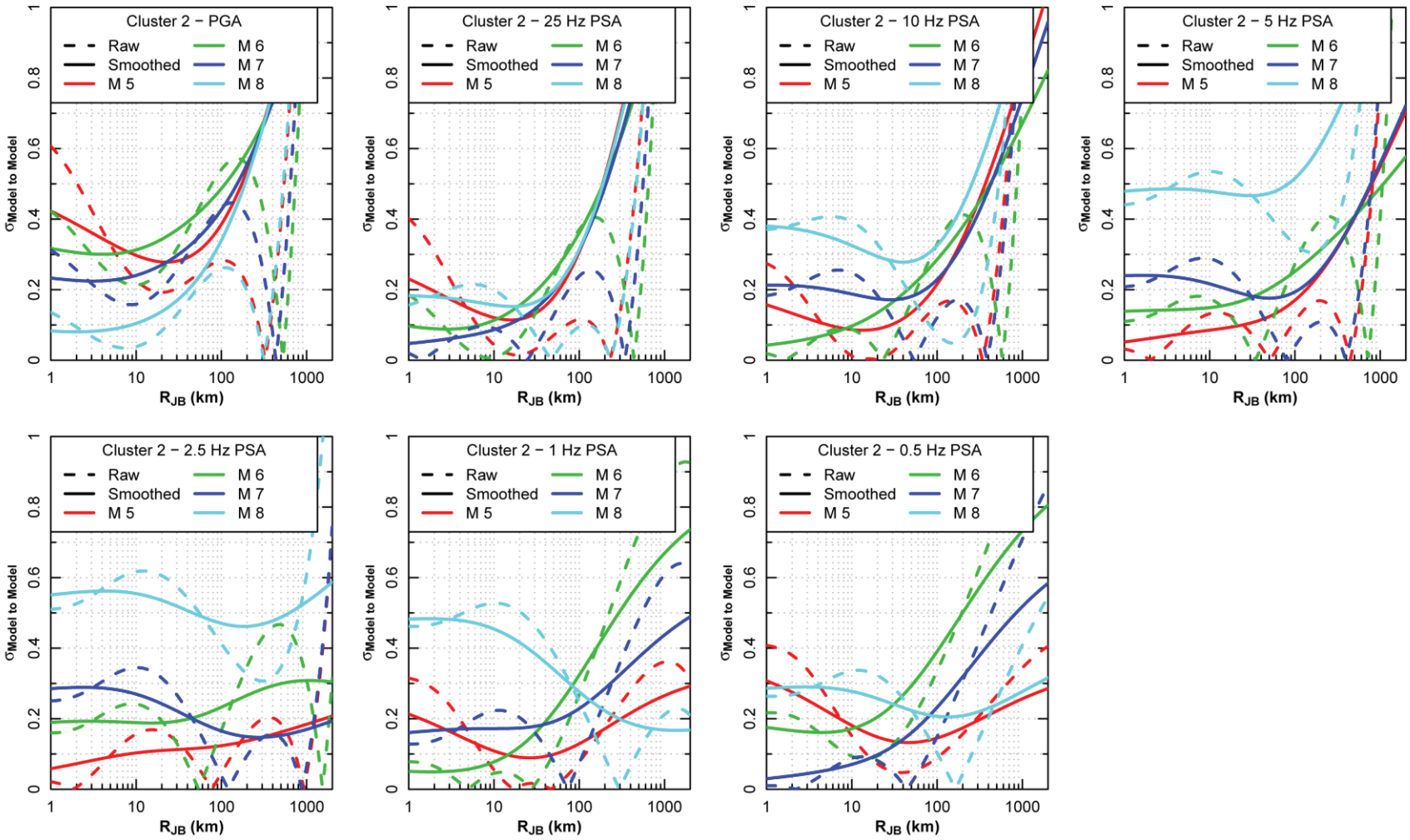

Figure 7.7.1-2
Model-to-model variability for Cluster 2

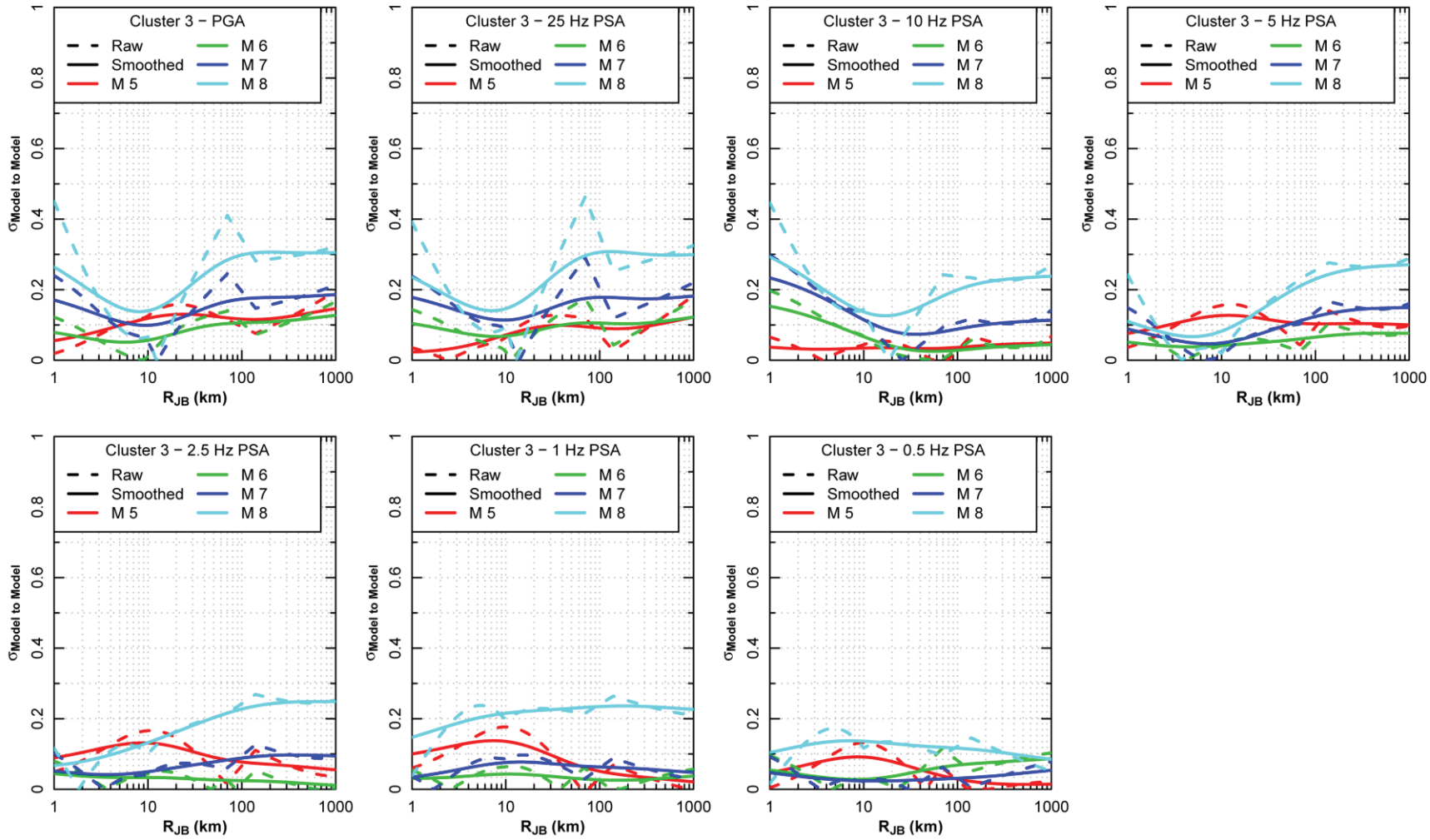

Figure 7.7.1-3
Model-to-model variability for Cluster 3

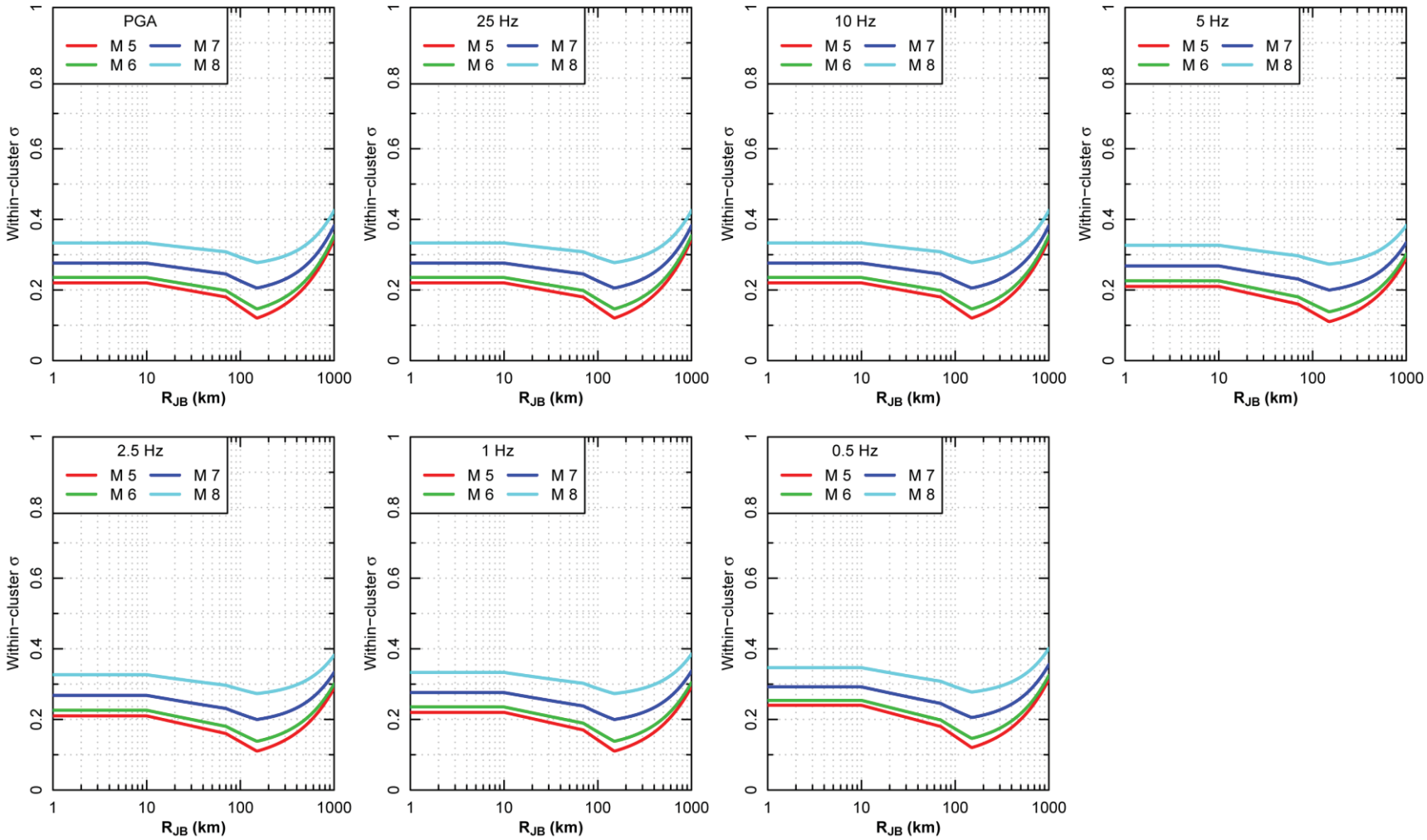

Figure 7.7.1-9
Cluster-independent values of within-cluster epistemic standard deviation

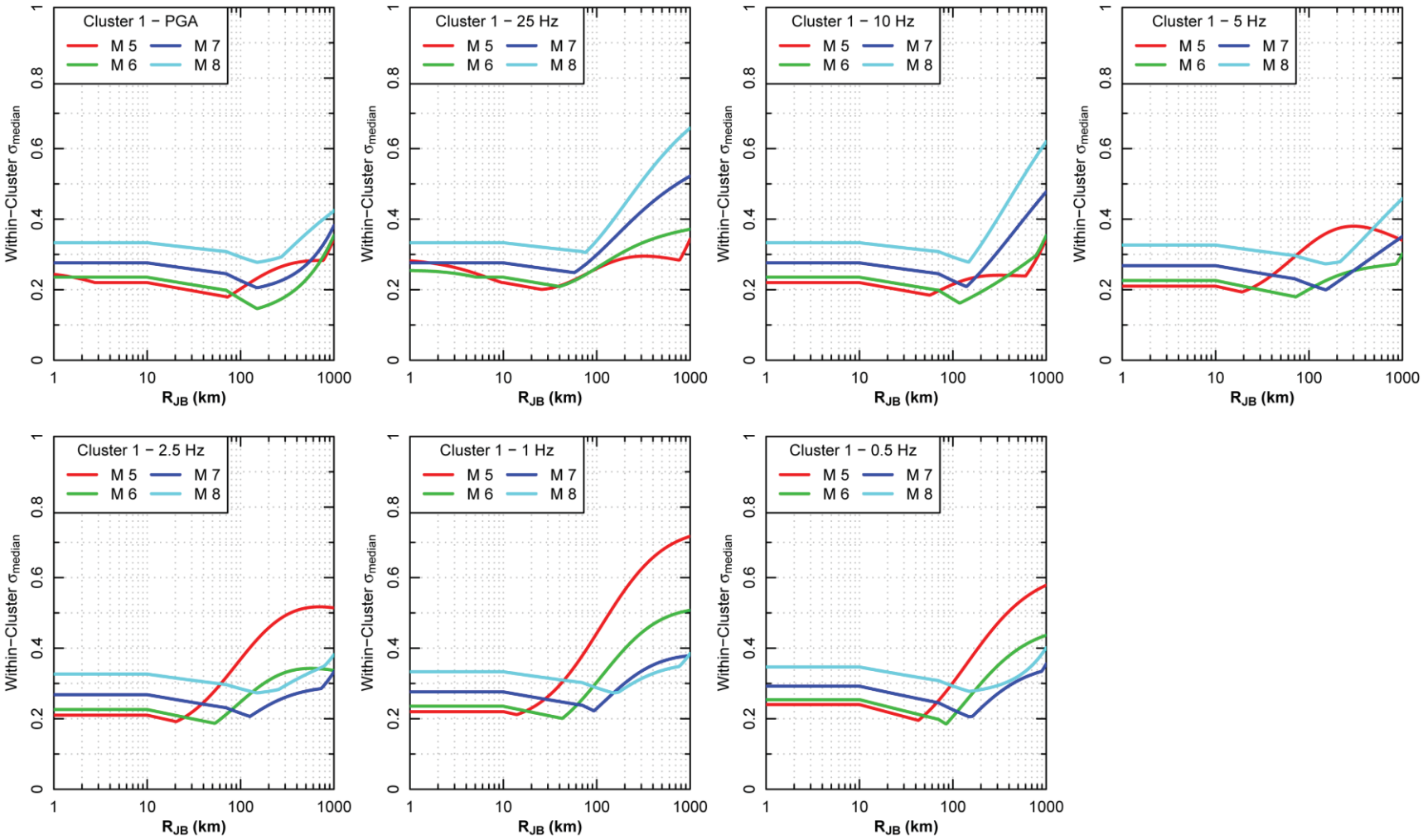

Figure 7.7.1-10
Within-cluster epistemic standard deviation of the median ground motions for Cluster 1

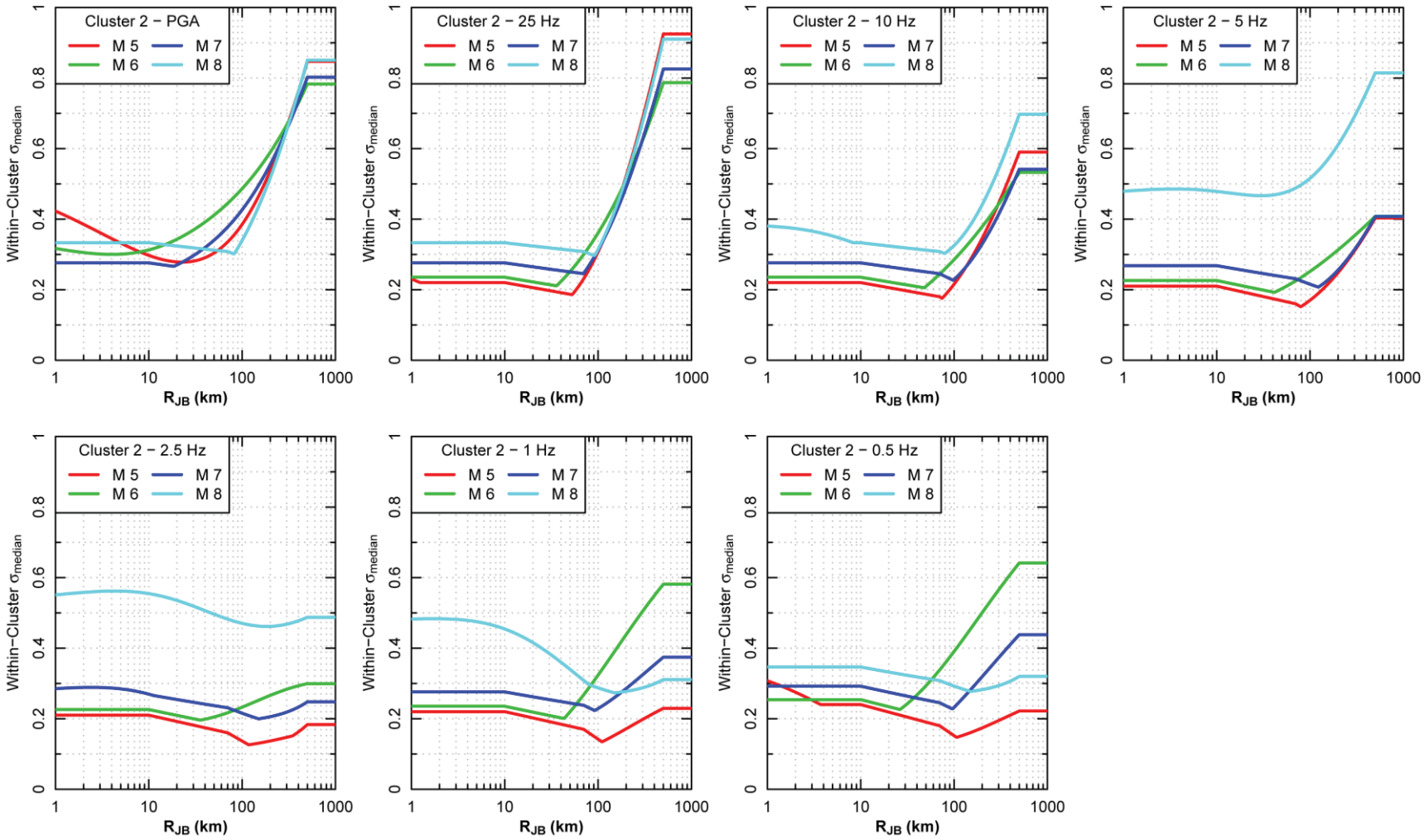

Figure 7.7.1-11
Within-cluster epistemic standard deviation of the median ground motions for Cluster 2

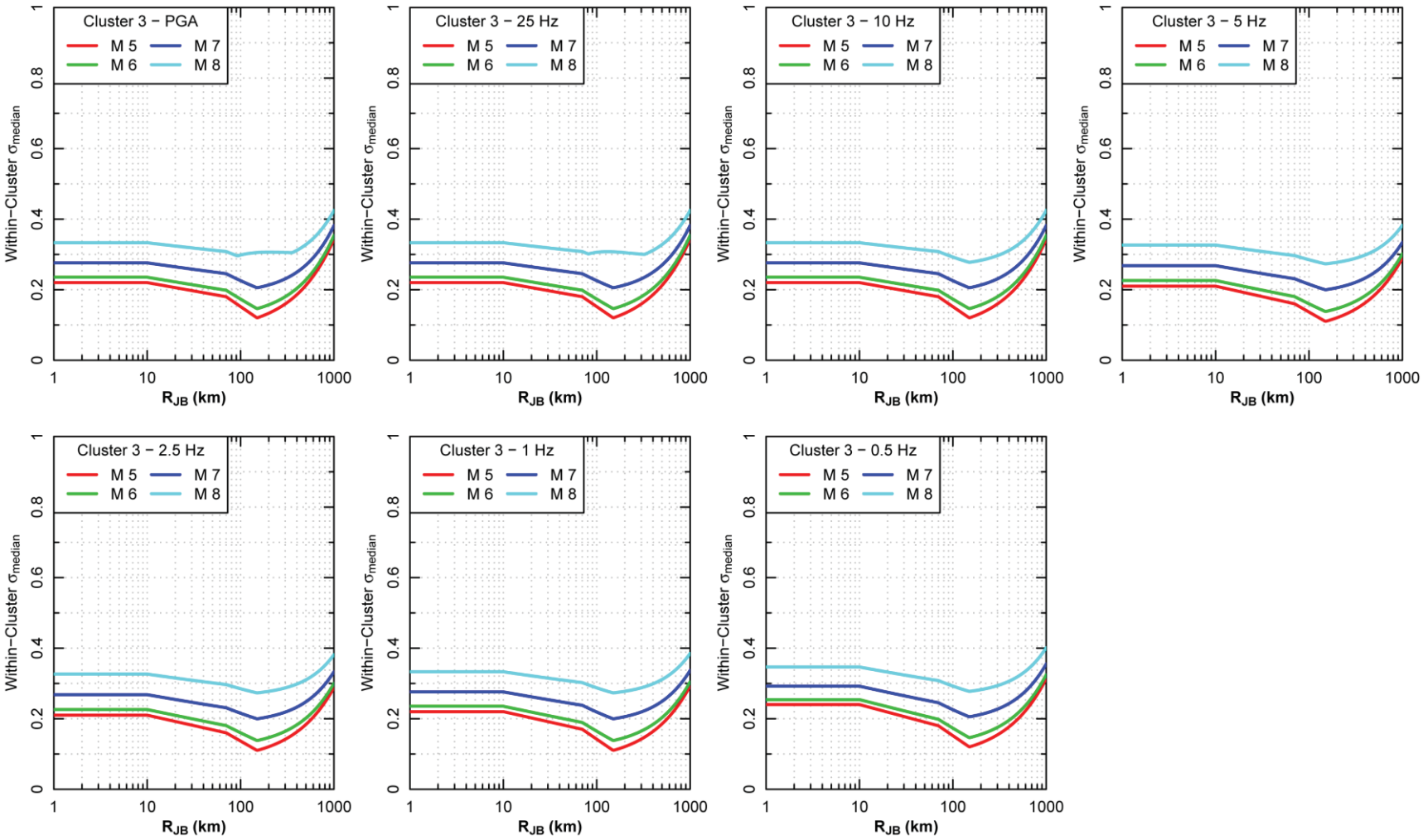

Figure 7.7.1-12
Within-cluster epistemic standard deviation of the median ground motions for Cluster 3

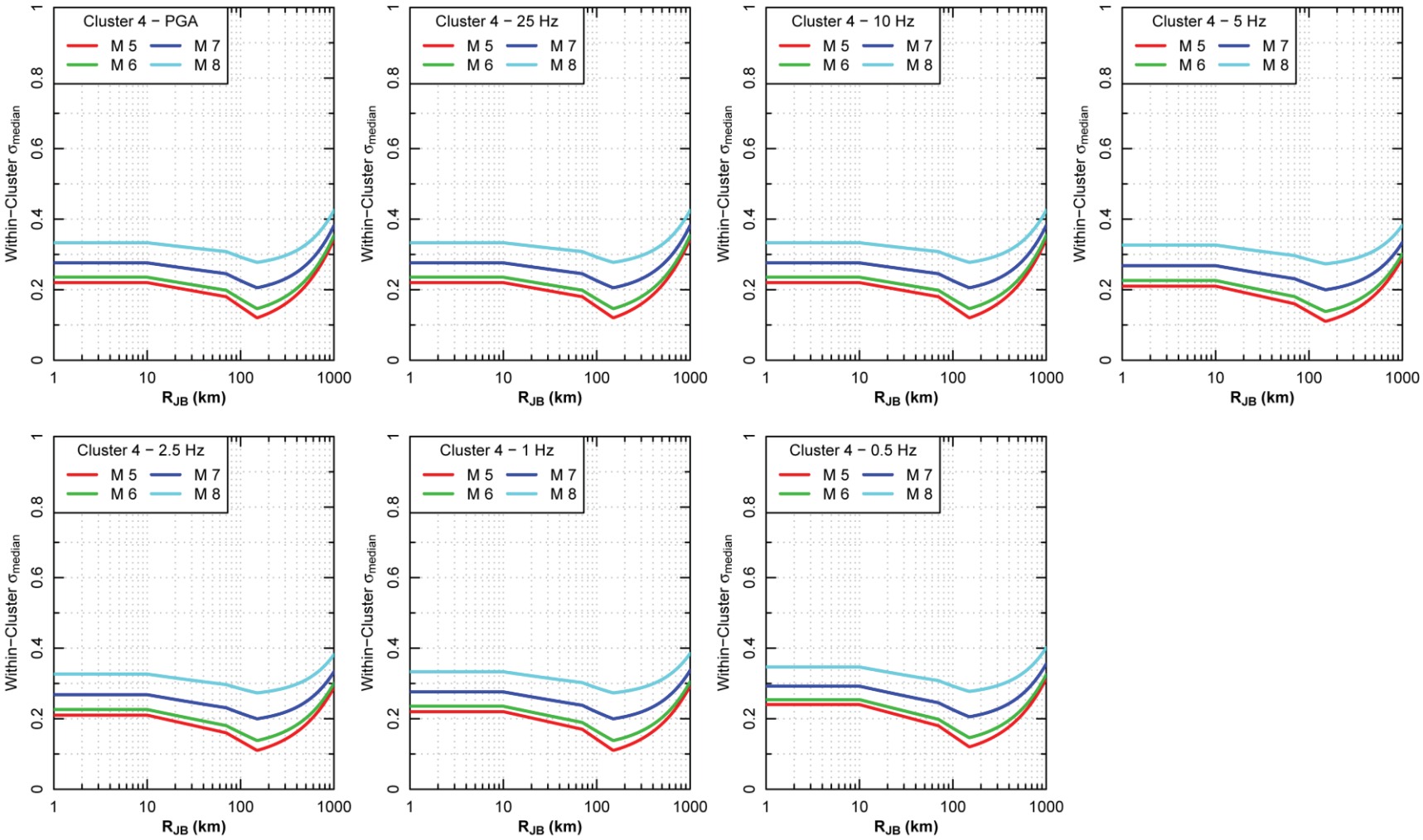

Figure 7.7.1-13
Within-cluster epistemic standard deviation of the median ground motions for Cluster 4

Question 8: Table A.6-1 contains the information on the ~1,890 recordings used in this project. The unadjusted PGA and SA values are contained in this flat-file. Table A.6-4 contains the analytically adjusted PGA and SA values for the approximately 90 recordings obtained at stations where shear-wave profiles exist and the analytical adjustment could be performed. By simply taking the ratios of these values the analytical adjustment factors can be obtained. However, no comparable table of the empirically adjusted spectral accelerations is provided. Please provide the flat-file for the empirically adjusted spectral accelerations.

Response:

Empirically adjusted ground-motion values for the soft-rock sites can be obtained using the soft-rock scaling factors listed in Table 7.5.2-1 of the report. The table contains the soft-rock scaling factor and its uncertainty computed for each of the nine GMPEs used in the development of the updated GMM. The scaling factors listed in the table represent the amplification of the soft-rock sites relative to the intermediate and very firm sites. The corresponding adjusted ground motions can be obtained by multiplying the values listed in Table A.6-1 by the factor $\exp[-C_{SR}]$ for those sites flagged as soft-rock sites. See Ground Motion Flat Files Folder; Project_Database/Table_A_6-1.xlsx for Table A.6-1.

A similar process was used to compute soft-rock scaling factors for each of the new cluster median models as part of the development of cluster weights. Table 8-1 below lists the soft-rock scaling factors computed for each of the cluster median models of the updated GMM. Note that the values for Cluster 4 are the same as those for the Somerville et al. (2001) model (SEL) in Table 7.5.2-1, as this is the only GMPE in Cluster 4.

Tables Cited in the Response

Table 7.5.2-1
Soft-Rock Scaling Factors Used for Empirical Site Adjustments

GMPE	Soft-Rock Scaling Factor C_{SR} for Frequency of:					
	25 Hz	**10 Hz**	**5 Hz**	**2.5 Hz**	**1 Hz**	**0.5 Hz**
SSCCSC	0.43 ± 0.17	0.11 ± 0.14	0.09 ± 0.13	0.25 ± 0.13	0.34 ± 0.13	0.59 ± 0.12
SSCVS	0.44 ± 0.17	0.10 ± 0.14	0.09 ± 0.13	0.25 ± 0.13	0.34 ± 0.12	0.59 ± 0.12
TEL	0.44 ± 0.16	0.12 ± 0.13	0.12 ± 0.13	0.27 ± 0.12	0.34 ± 0.11	0.57 ± 0.11
FEL	0.46 ± 0.16	0.16 ± 0.13	0.15 ± 0.12	0.30 ± 0.12	0.36 ± 0.11	0.58 ± 0.11
A08′	0.35 ± 0.15	0.16 ± 0.13	0.15 ± 0.12	0.29 ± 0.11	0.34 ± 0.12	0.60 ± 0.11
SDCS	0.44 ± 0.17	0.11 ± 0.14	0.10 ± 0.13	0.25 ± 0.13	0.34 ± 0.13	0.59 ± 0.12
AB06′	0.50 ± 0.17	0.19 ± 0.14	0.16 ± 0.13	0.30 ± 0.12	0.35 ± 0.12	0.56 ± 0.11
PZT	0.49 ± 0.17	0.20 ± 0.15	0.17 ± 0.13	0.31 ± 0.12	0.36 ± 0.12	0.56 ± 0.11
SEL	0.43 ± 0.18	0.18 ± 0.14	0.16 ± 0.12	0.31 ± 0.12	0.38 ± 0.13	0.63 ± 0.13

Table 8-1
Soft-Rock Scaling Factors Used for Empirical Site Adjustments for the Cluster Median Models

GMPE	Soft-Rock Scaling Factor C_{SR} for Frequency of:					
	25 Hz	**10 Hz**	**5 Hz**	**2.5 Hz**	**1 Hz**	**0.5 Hz**
Cluster 1	0.45 ± 0.17	0.12 ± 0.13	0.11 ± 0.13	0.27 ± 0.12	0.35 ± 0.12	0.59 ± 0.11
Cluster 2	0.39 ± 0.15	0.14 ± 0.13	0.12 ± 0.13	0.27 ± 0.12	0.34 ± 0.12	0.58 ± 0.11
Cluster 3	0.48 ± 0.16	0.18 ± 0.14	0.16 ± 0.13	0.30 ± 0.12	0.35 ± 0.12	0.56 ± 0.11
Cluster 4	0.43 ± 0.18	0.18 ± 0.14	0.16 ± 0.12	0.31 ± 0.12	0.38 ± 0.13	0.63 ± 0.13

APPENDIX

Errata for EPRI Technical Report
EPRI (2004, 2006) Ground-Motion Model (GMM) Review Project
3002000717, June 2013